

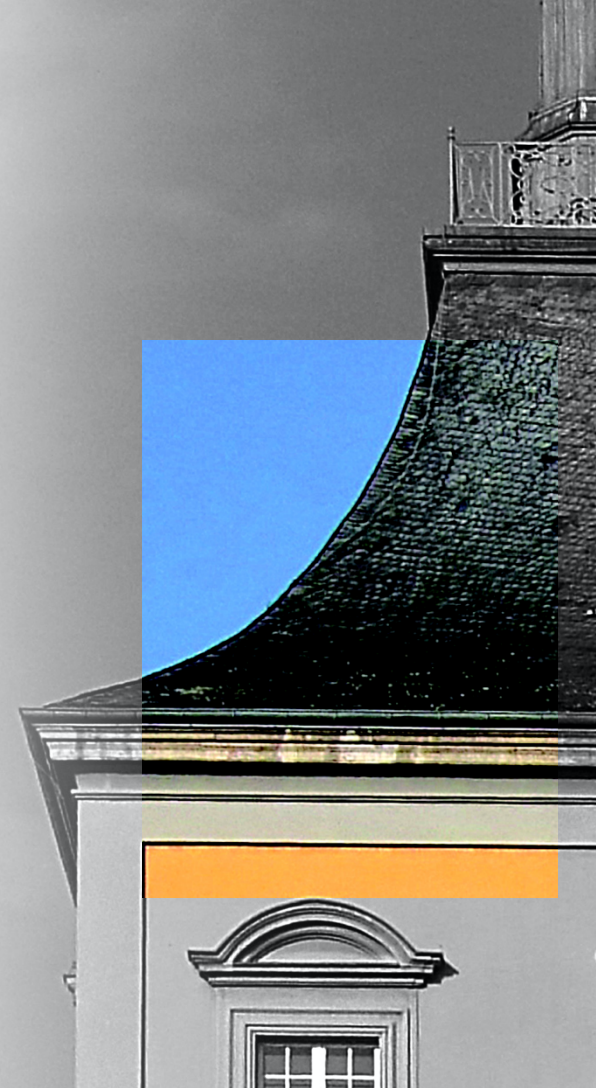
SIGNAL FORMATION AND SIGNAL PROCESSING IN DETECTORS

LECTURES AT THE UNIVERSITY OF FREIBURG

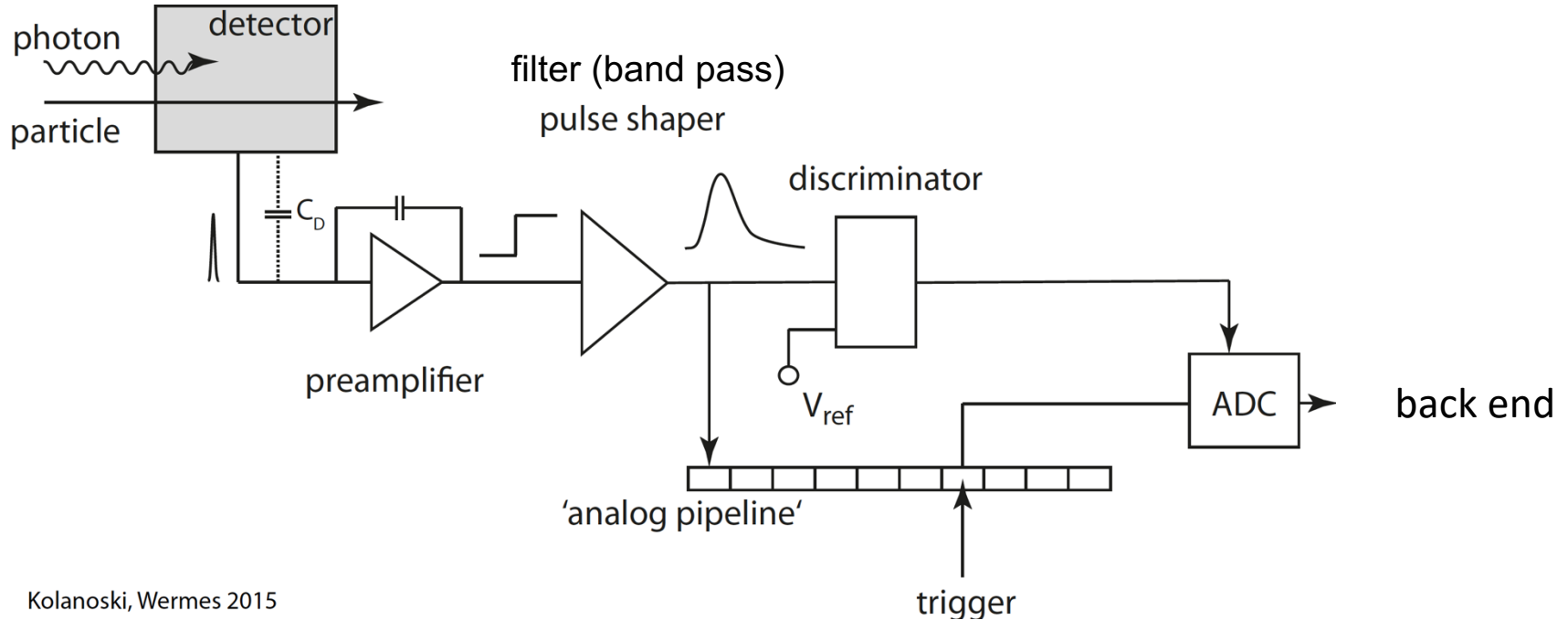
MARCH 9-14, 2020

LECTURE 2

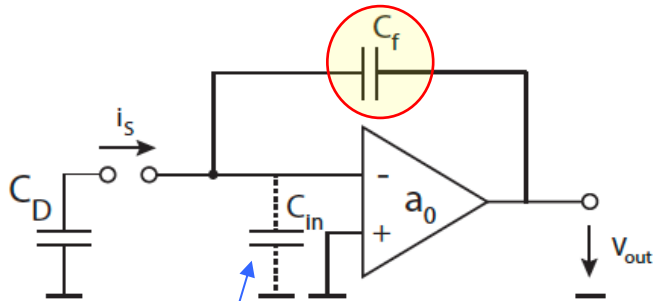
NORBERT WERMES
UNIVERSITY OF BONN



1. What is a detector “signal”?
2. Charge transport in gases and solids
3. Induced signals on electrodes
 - Schottky-Ramo Theorem
 - Current, charge or voltage?
 - Applying Ramo to detectors
 - Structured electrodes
 - (calculation of E_W by “conformal mapping”)
4. Signal fluctuations and (electronic) noise
 - Why bother?
 - Signal fluctuations (Fano noise)
 - Electronic noise
5. Readout of signals
 - • Amplification
 - (Excursion: Laplace transform)
 - Filtering
 - Discrimination
 - Digitisation
 - (Example: a readout chip)
6. Signal transmission off detector
7. Noise of a readout system
 - Explicit calculation of noise
 - ATLAS pixel detector
 - ATLAS strip detector
 - ATLAS Liq. Argon calorimeter



Kolanoski, Wermes 2015



(b) Capacitive feedback.

$$C_{in} = C_f (a_0 + 1)$$

dynamic input capacitance

(should be very large, else C_D incompletely discharged => unwanted x-talk possible)

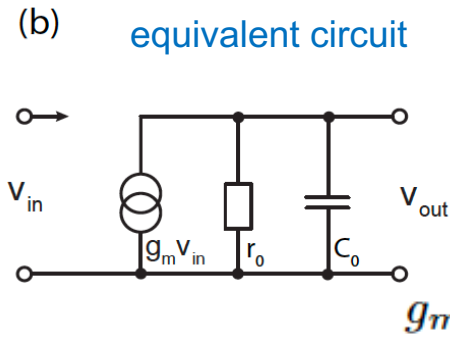
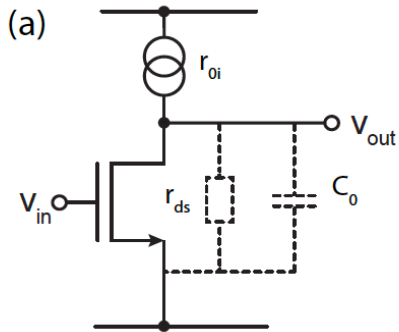
charge (sensitive) amplifier (CSA)
(= current integrator)

The signal current is integrated on C_f

$$v_{out}(t) = -a_0 v_{in}(t) = -\frac{1}{C_f} \int_0^t i_S dt' = -\frac{Q_S(t)}{C_f}$$

$$A_Q = \left| \frac{v_{out}}{Q_S} \right| \approx \frac{1}{C_f}$$

gain



$$a(\omega) = -\frac{v_{out}}{v_{in}} = -\frac{i_{out}}{v_{in}} \cdot (r_0 \parallel C_0)$$

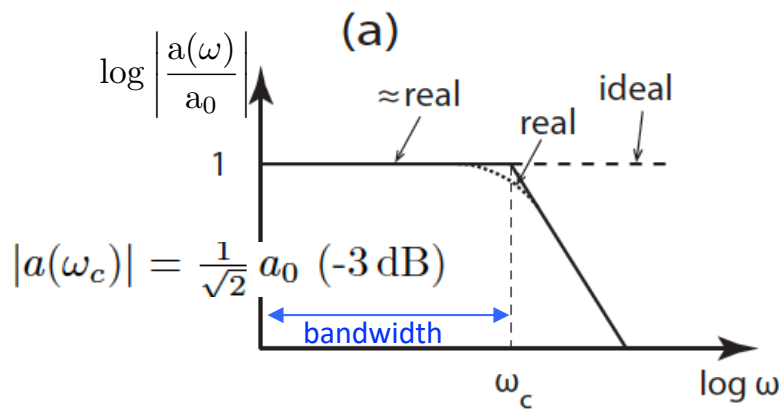
$$= -g_m \frac{r_0}{1 + i\omega r_0 C_0} = \frac{a_0}{1 + i\frac{\omega}{\omega_c}}$$

transfer function

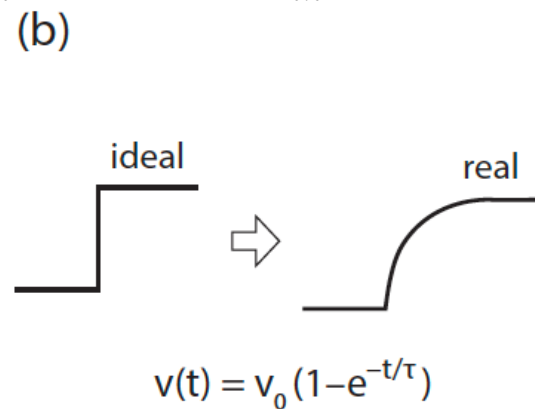
$\omega_c = \frac{1}{r_0 C_0}$

$$a_0 = -\frac{v_{out}}{v_{in}} (\omega \rightarrow 0) = -\frac{i_{out}}{v_{in}} r_0 = -g_m r_0$$

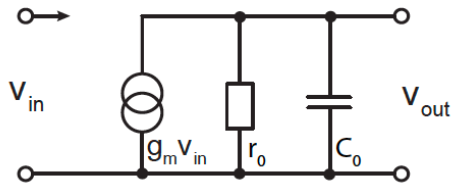
Bode Plot



frequency domain

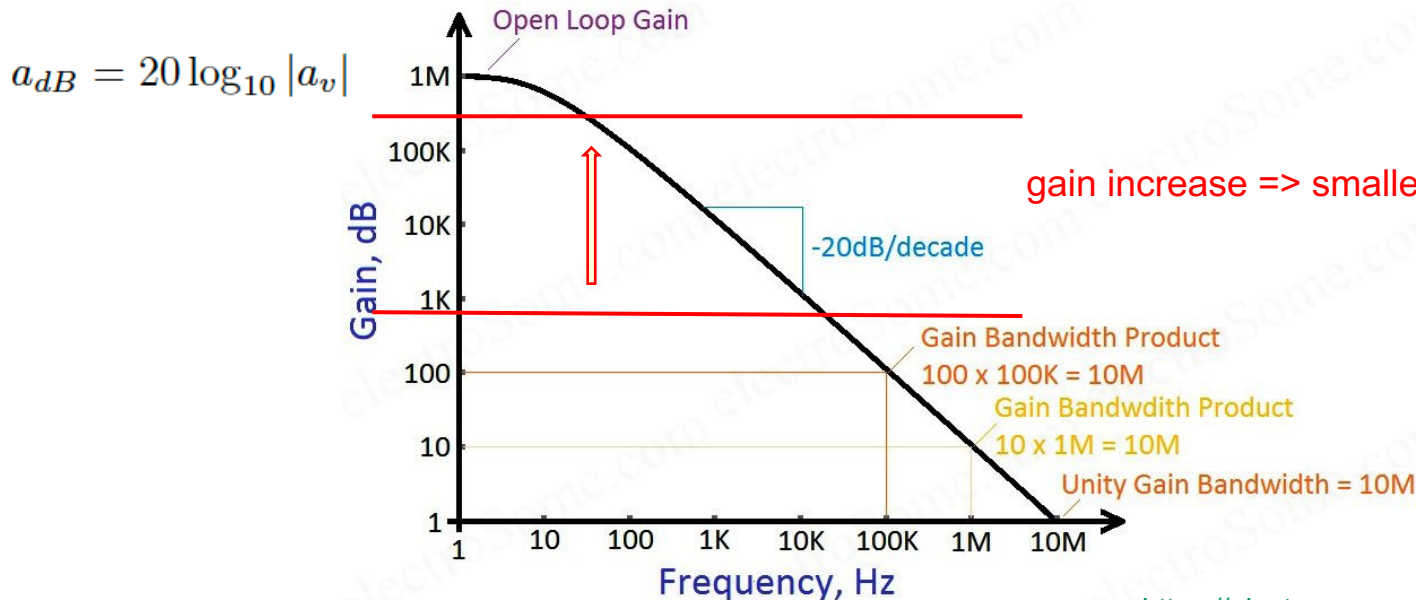


time domain



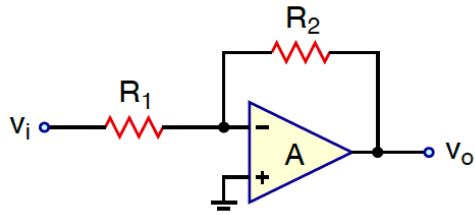
$$GBP = |a(\omega) \times \omega| \approx g_m r_o \cdot \frac{1}{r_o C_0} = \frac{g_m}{C_0}$$

≈ **CONST** ! (for a single stage, single pole amplifier)

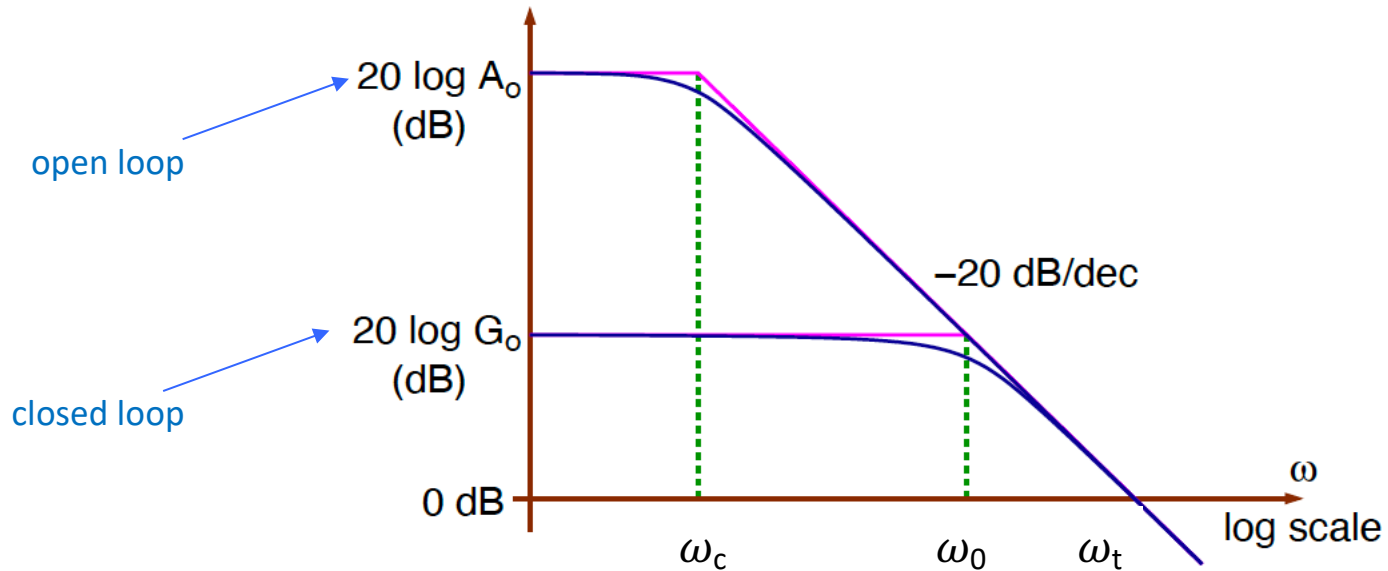


gain increase => smaller BW => slower response

Reducing the gain => increasing the BW



e.g. by (inverted) feedback



remember dyn. C_{in}

$$C_{in} = \frac{Q_S}{v_{in}} = C_f (a_0 + 1)$$

$$\Rightarrow Z_{in}(f) = \frac{1}{i\omega C_{in}} = \frac{1}{(a(\omega) + 1) \cdot i\omega C_f} \approx \frac{1}{ia(\omega) \omega C_f}$$

at low frequencies

$$a(\omega) \rightarrow a_0 \Rightarrow Z_{in}(\omega) \rightarrow \frac{1}{ia_0 \omega C_f} \quad \text{behaves as a capacitor}$$

$$a(\omega) = \frac{a_0}{1 + i \frac{\omega}{\omega_c}}$$

$$\Rightarrow a(\omega) \rightarrow -ia_0 \frac{\omega_c}{\omega} \Rightarrow Z_{in}(\omega) \rightarrow \frac{1}{(-ia_0 \frac{\omega_c}{\omega}) \cdot i\omega C_f}$$

at high frequencies

$$= \frac{1}{a_0 \omega_c C_f} = \frac{1}{\text{GBP} \cdot C_f} = \frac{C_0}{C_f} \frac{1}{g_m} = R_{in}$$

$C_0 = \text{cap. of amplifier}$

behaves as a resistor, since $g_m \triangleq 1/R$

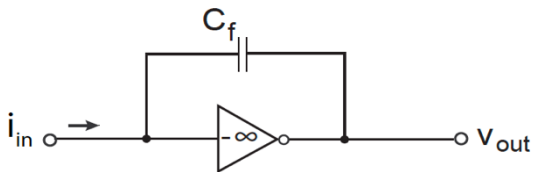
\Rightarrow “timing”

$$\tau_{CSA} = C_D R_{in} = \frac{C_D}{C_f} \frac{1}{a_0 \omega_c} = \frac{C_D}{C_f} \frac{C_0}{g_m}$$

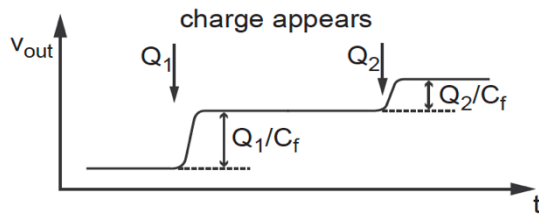
det. capacitance

power

ideal situation w/o reset

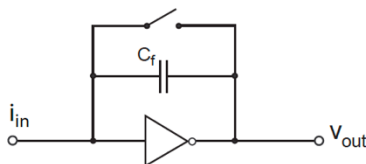


(a) Circuit diagram.

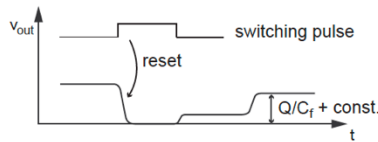


(b) Output voltage.

=> "pile-up" => saturation



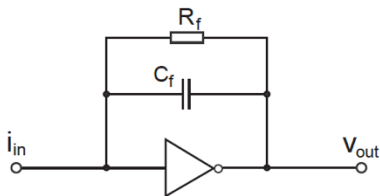
(a) Switch reset: circuit.



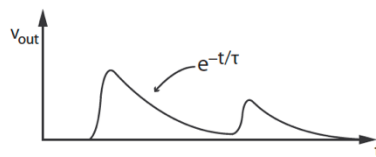
(b) Switch reset: output voltage.

"reset" switch

discharging options

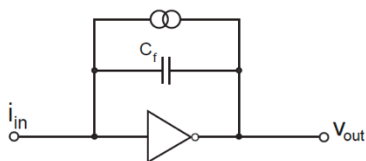


(c) Reset via resistor: circuit.

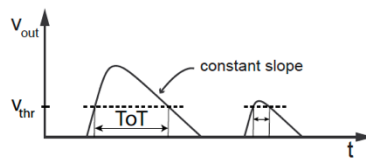


(d) Reset via resistor: output voltage.

resistor R_f



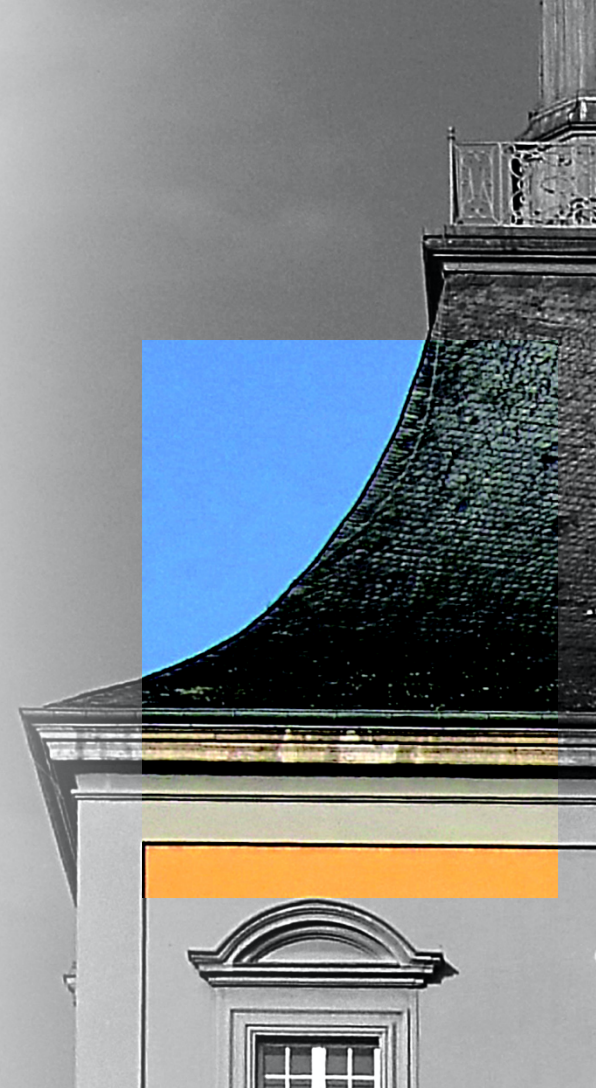
(e) Reset via current source: circuit diagram.



(f) Reset via current source: output voltage.

a current source

Short excursion: Laplace Transform



- Convenient method to switch from time to frequency domain and back.
- Very similar to Fourier transform (Laplace encompasses Fourier)

$$F(s) = \mathcal{L}[f(t)] = \int_0^{\infty} f(t) e^{-st} dt,$$

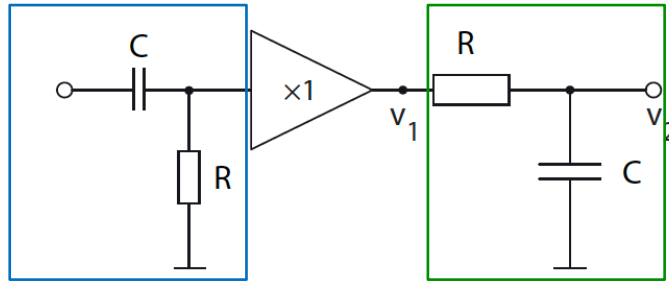
$$s = \sigma + i\omega$$

σ = a constant generating convergence for time-wise constraint functions

$$\mathcal{L}^{-1}[F(s)] = \frac{1}{2\pi i} \int_{\sigma-i\infty}^{\sigma+i\infty} F(s) e^{st} ds = \begin{cases} f(t) & \text{for } t \geq 0 \\ 0 & \text{for } t < 0 \end{cases}$$

Operation or function	Time domain	Frequency domain
	$f(t) = \mathcal{L}^{-1}[F(s)]$	$F(s) = \mathcal{L}[f(t)]$
linearity	$a_1 f_1(t) + a_2 f_2(t)$	$a_1 F_1(s) + a_2 F_2(s)$
convolution	$\int_0^\infty f(t-t')g(t')dt'$	$F(s)G(s)$
<i>n</i> th derivative	$\frac{d^n}{dt^n} f(t)$	$s^n F(s)$
time integration	$\int_0^t f(t)dt$	$\frac{1}{s} F(s)$
scaling of <i>t</i>	$f(at)$	$\frac{1}{a} F\left(\frac{s}{a}\right)$
time shift	$f(t-t_0)$	$e^{-st_0} F(s)$
damping	$e^{-s_0 t} f(t)$	$F(s+s_0)$
multiplication	$t^n f(t)$	$(-1)^n \frac{d^n}{ds^n} F(s)$
δ function	$\delta(t)$	1
derivative of the δ function	$\frac{d^n}{dt^n} \delta(t)$	s^n
step function	$\Theta(t)$	$\frac{1}{s}$
falling exponential	e^{-at}	$\frac{1}{s+a}$
rising exponential	$1 - e^{-at}$	$\frac{a}{s(s+a)}$
power function	t^n	$\frac{n!}{s^{n+1}}$





transfer function:

$$H(s) = \frac{v_{out}(s)}{v_{in}(s)}$$

voltage divider

$$\frac{v_{out}(t)}{v_{in}(t)} = \frac{i(t)R}{\frac{1}{C} \int i(t)dt + i(t)R}$$



$$\frac{v_{out}(s)}{v_{in}(s)} = \frac{i(s)R}{\frac{1}{sC}i(s) + i(s)R}$$



$$H_1(s) = \frac{sRC}{1 + sRC}$$

$$H_2(s) = \frac{1}{1 + sRC}$$

$$\Rightarrow \text{CR-RC: } H(s) = H_1(s) \times H_2(s)$$

$$v_1(s) = H_1(s) v(s) = \frac{sRC}{1 + sRC} v(s) = \frac{s\tau}{1 + s\tau} v(s),$$

$$v_2(s) = H_2(s) v_1(s) = \frac{1}{1 + sRC} v_1(s) = \frac{s\tau}{(1 + s\tau)^2} v(s)$$

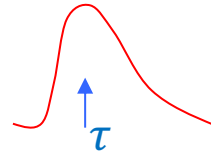
step function input

$$v(t) = V_0 \Theta(t) \Rightarrow v_2(s) = \frac{V_0 \tau}{(1 + s\tau)^2} \Rightarrow v_2(t) = V_0 \frac{t}{\tau} e^{-t/\tau}$$

necessary

- (i) to avoid pile-up of signals
- (ii) to reduce the bandwidth => reduce noise (see later)

in time domain



$$v_{sh}(t) = A \frac{t}{\tau} e^{-\frac{t}{\tau}}$$

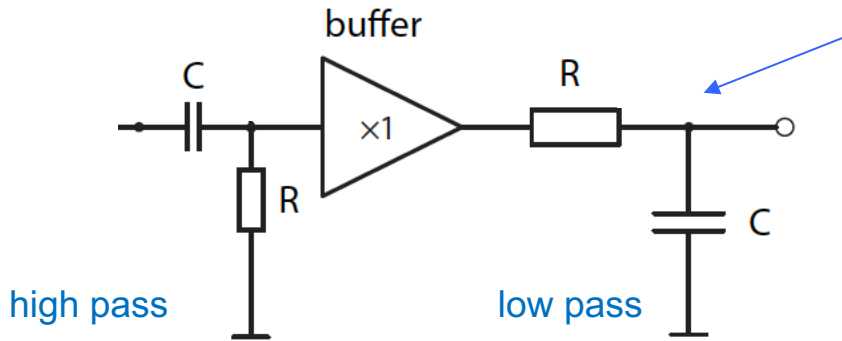
peaking at τ with $v(\tau) = A / 2.71$

in frequency domain

$$1/s$$



$$H(s) = A \frac{s\tau}{(1 + s\tau)^2}$$



usually realised as
CR – RC shaper

$$A(t) = \frac{t}{\tau} e^{-\frac{t}{\tau}}$$

or as

(CR)^N – (RC)^M shaper

$$A(t) = \frac{1}{M!} \left(\frac{t}{\tau}\right)^M e^{-\frac{t}{\tau}}$$

for N = 1

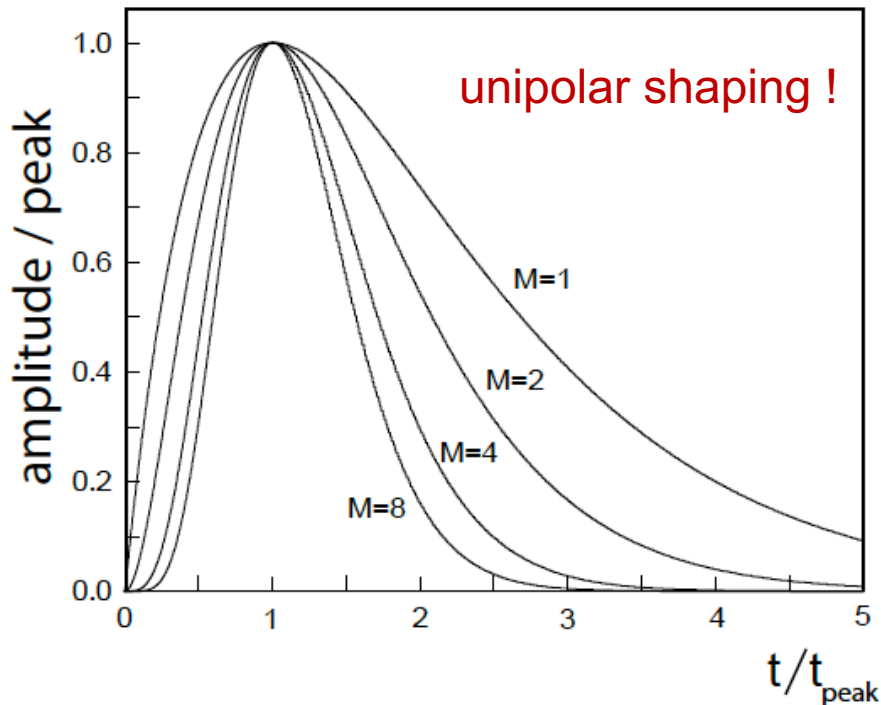


Fig. 17.12 Step response output of CR-(RC)^M shaper stages of different order *M*. Amplitudes and times are normalised to their respective peak amplitude.

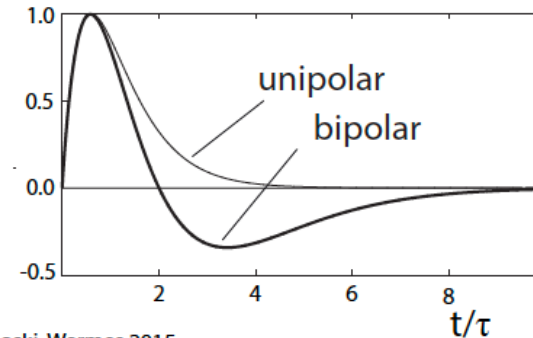
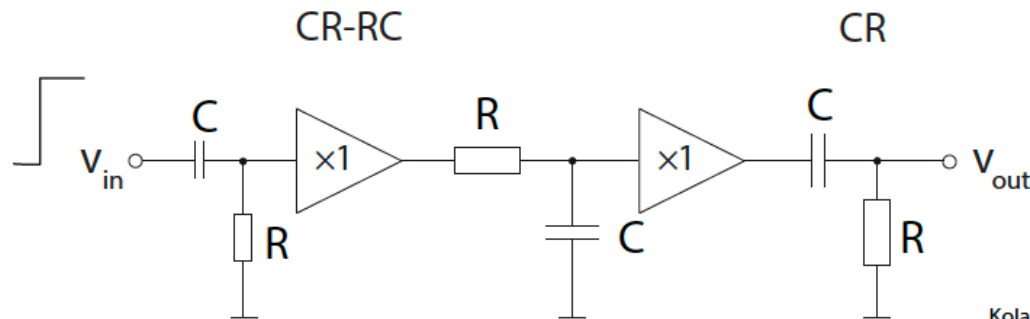
With increasing *M*

=> shape more Gaussian and, if one chooses a shorter peaking time, also narrower in absolute terms.

=> better double-pulse resolution

However, the electronic effort is substantially larger than for CR-RC shapers.

By adding a further high-pass filter to any unipolar shaper a **bipolar** pulse shape is obtained with equal area in both wings. This can be done by adding a CR high-pass filter after M low-pass filters.



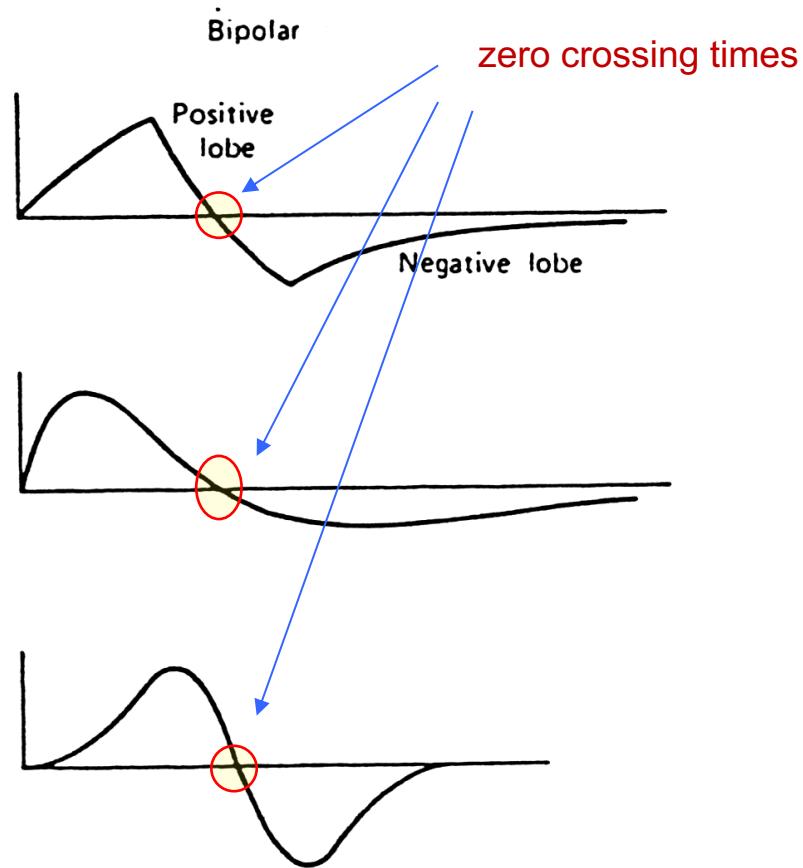
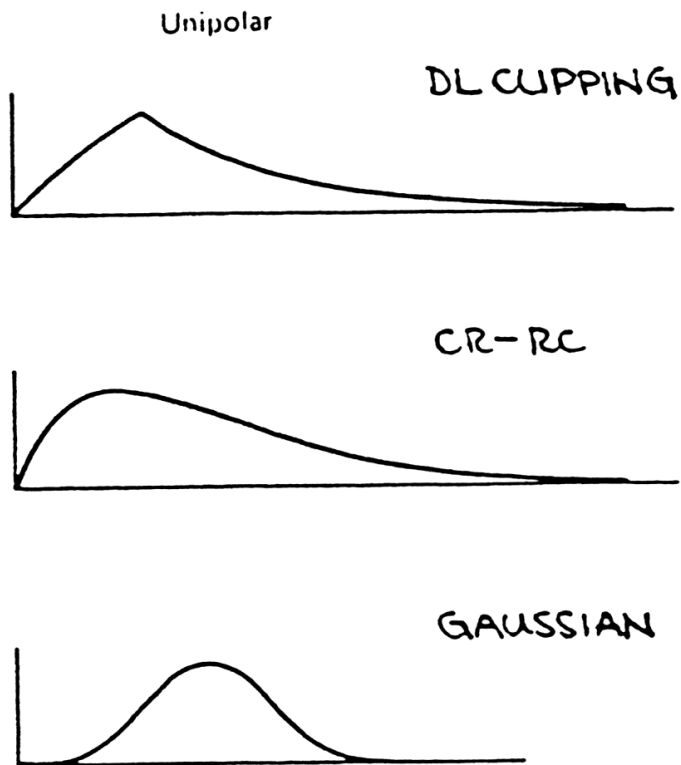
Kolanoski, Wermes 2015

advantages

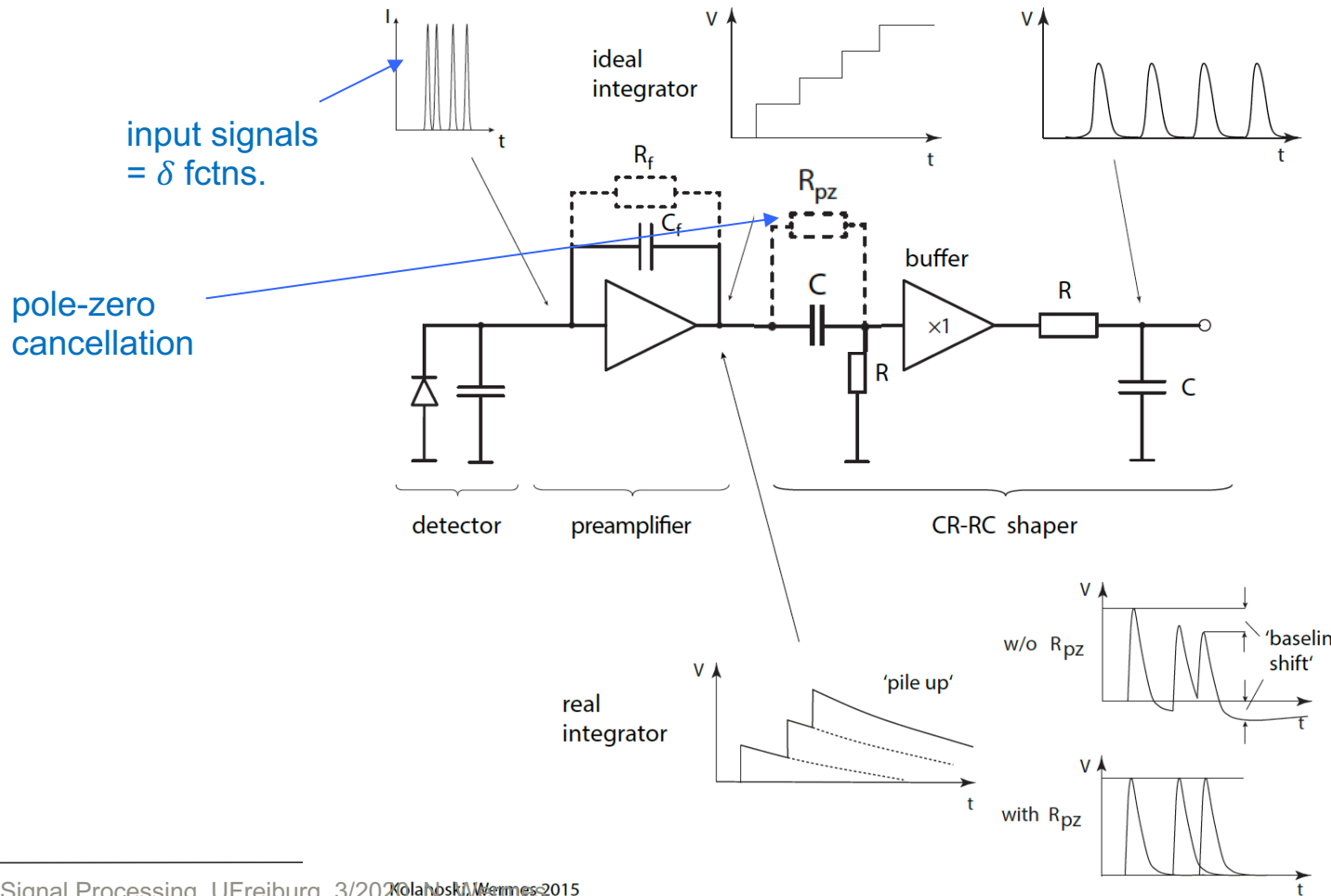
- digests high count rates
- is simple and robust against baseline fluct.
- is good for time-critical applications
(use zero-crossing time as observable)

less good

- somewhat more power consumption
- somewhat worse S/N
- needs larger chip area



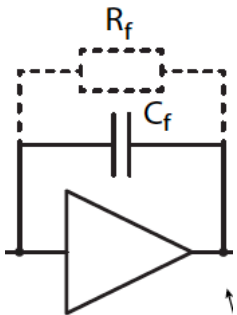
The amplifier system = preamp + shaper (= filter)



ideal

real

Without further corrections **unipolar shaping** also features **unwanted undershoots** in realistic applications. Origin is the (slow) discharge of the feedback capacitor C_f .

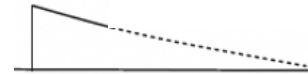
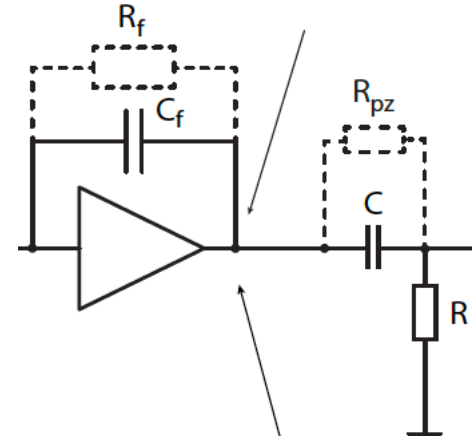


$$v_{out}(s) = \frac{R_f}{1 + s\tau_f} i_{in}(s)$$

pole on real axis for $s = \pm 1/\tau_f$
(resp. for Bode plot and position of ω_c)



works fine for a input ($1/s$), but not for a shaper no longer cancels the $1/s$ in the step function pulse, which leads to the undershoot



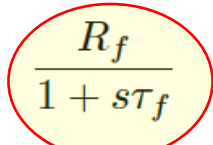
pulse, because the CR of the shaper no longer cancels the $1/s$ in the step function pulse, which leads to the undershoot

but with R_{pz}

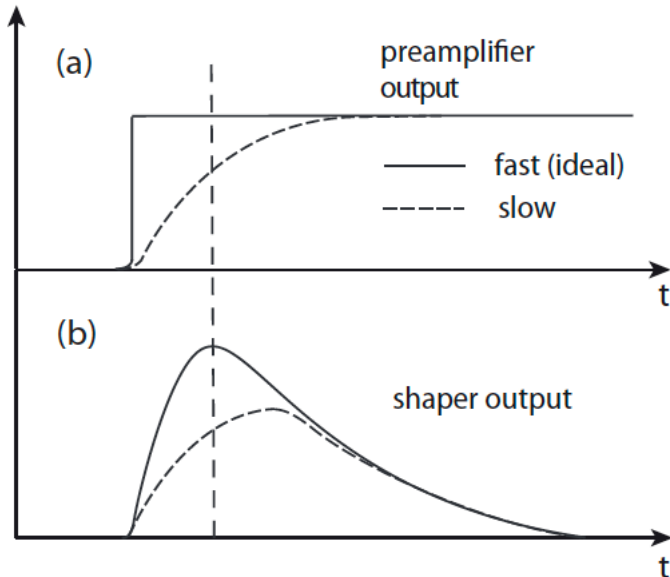
$$H(s) = H_{CSA}(s) \cdot H_{pz}(s) = \frac{R_f}{1 + s\tau_f} \cdot \frac{1 + s\tau_{pz}}{1 + \frac{R_{pz}}{R} + s\tau_{pz}}$$

$$\stackrel{\tau_{pz} = \tau_f}{=} \frac{R_f}{1 + \frac{R_{pz}}{R} + s\tau_f} \xrightarrow{R_{pz} \ll R} \frac{R_f}{1 + s\tau_f}$$

original $H(s)$ restored



“ballistic deficit” or “shaping loss”

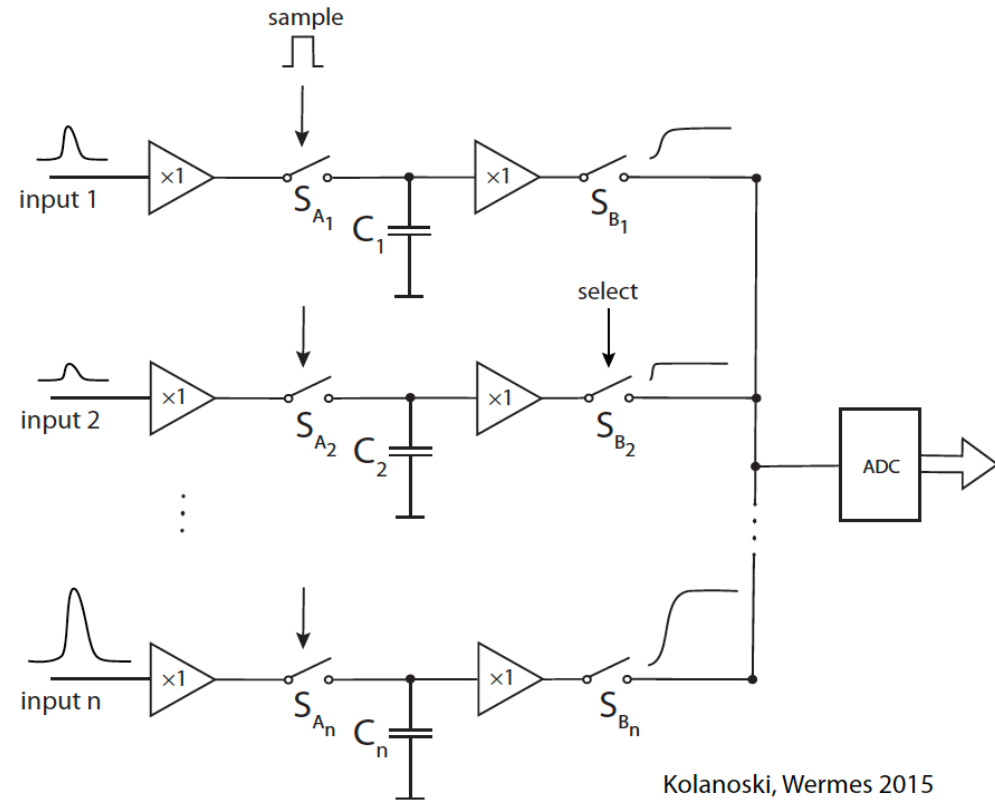


- If pulse evolution at the shaper input takes much longer than the shaper τ_{CR}
 - caused e.g.
 - by a large charge collection time
 - by a large input capacitance
 - by an intrinsically slow preamplifier.
- => The v_{out} (shaper) is trimmed by the slow rise of the preamplifier output pulse.
The falling edge of the shaper output already sets in before the preamplifier output has reached its maximum value.

skip S&H?

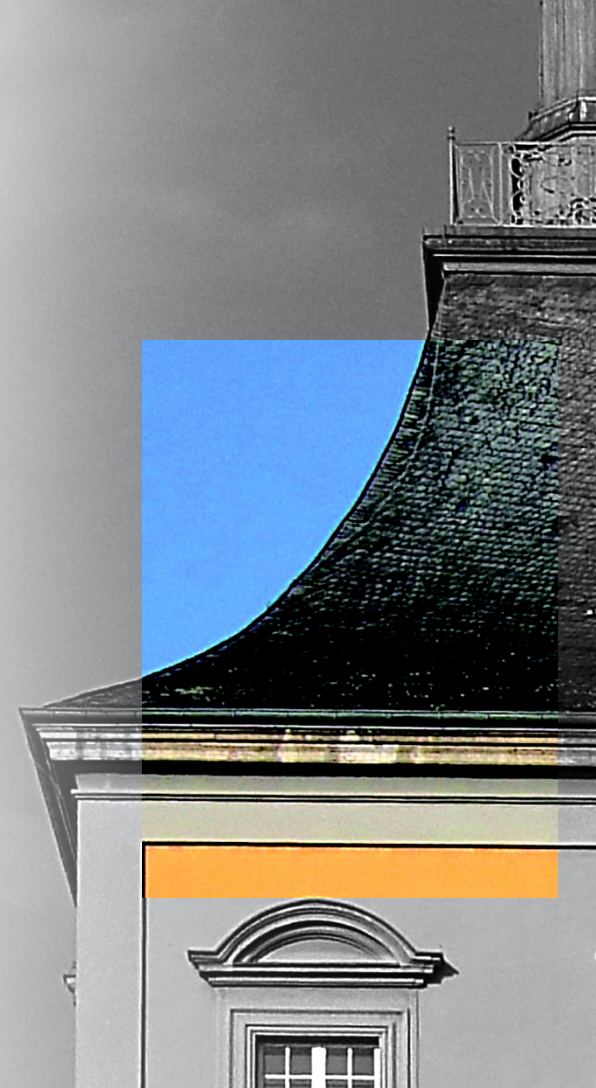


- If signal **shape and arrival time** are known
- \Rightarrow sample v_{in} at a fixed time, hold them for Δt , and process later
- **Sample pulse** (derived from trigger and delayed coincident with the peak) opens the switches S_A for sampling on the C_i .
- readout the switches S_B are successively closed, hence sequentially transferring the stored voltages serially onto the ADC
- By fast sampling the pulse in successive time intervals and storing the voltages in a series of sample-hold cells, called analog memory, one can memorise the whole pulse shape (**wave form sampling**).

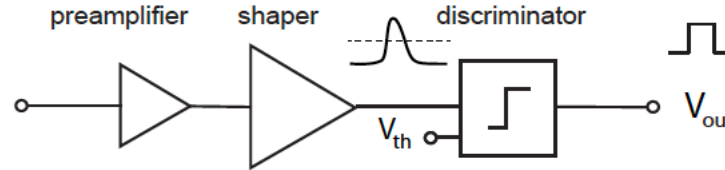


Kolanoski, Wermes 2015

The discriminator



= voltage comparator
needed to filter out
noise hits

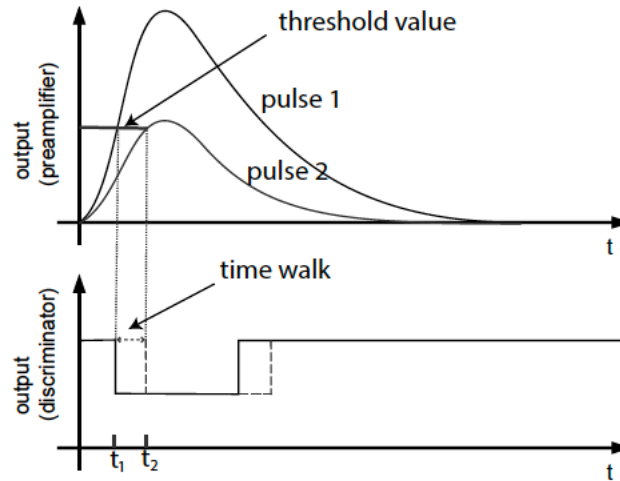


(a) Readout system with amplifier, shaper, and discriminator.

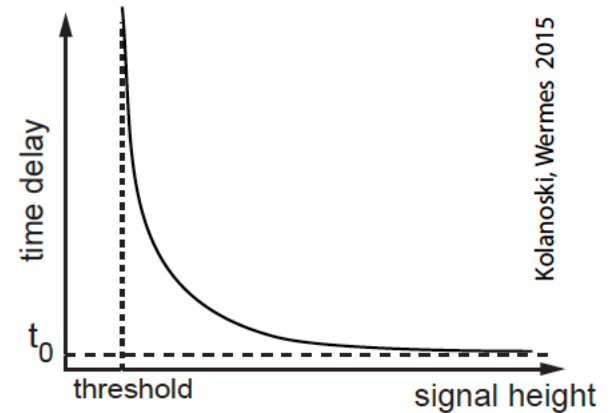
standard = leading edge discrimination

time
walk

typical: best timing
performance if
threshold at ~10-20%
of peak value
(depending on noise)



(b) Time walk.

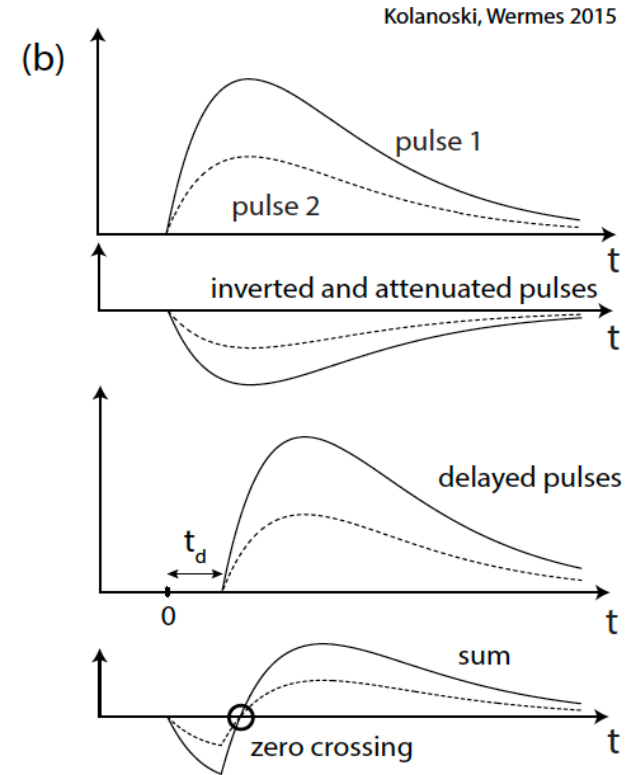
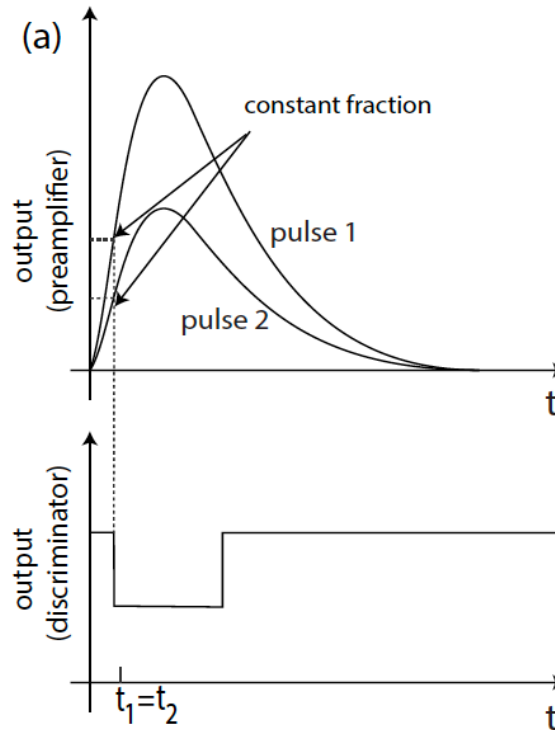


(c) Dependence of time walk on the signal pulse height (schematic).

Kolanoski, Wermes 2015

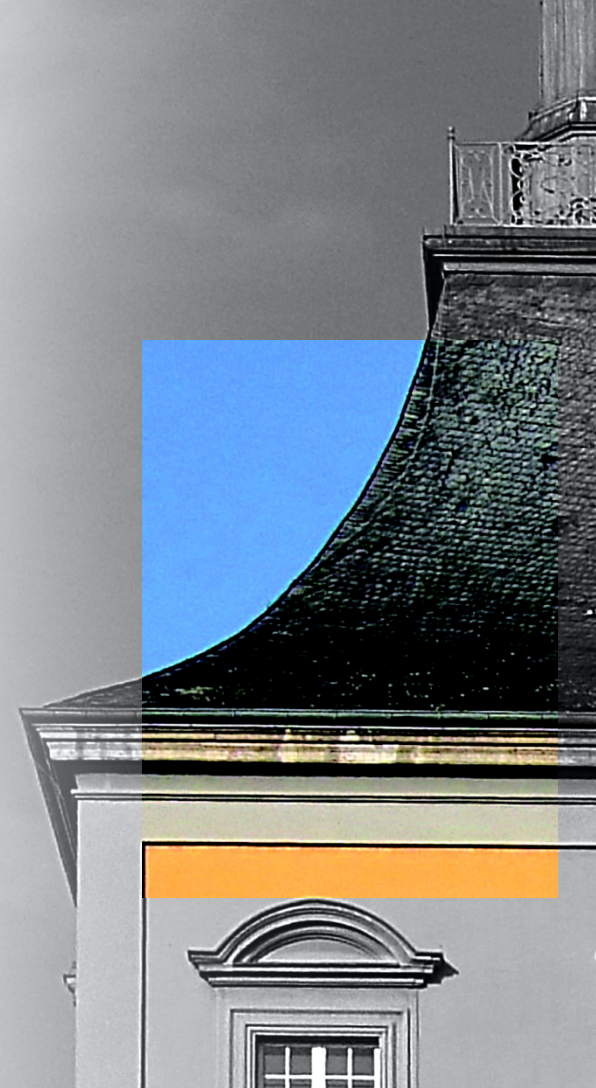
when stable timing is an issue

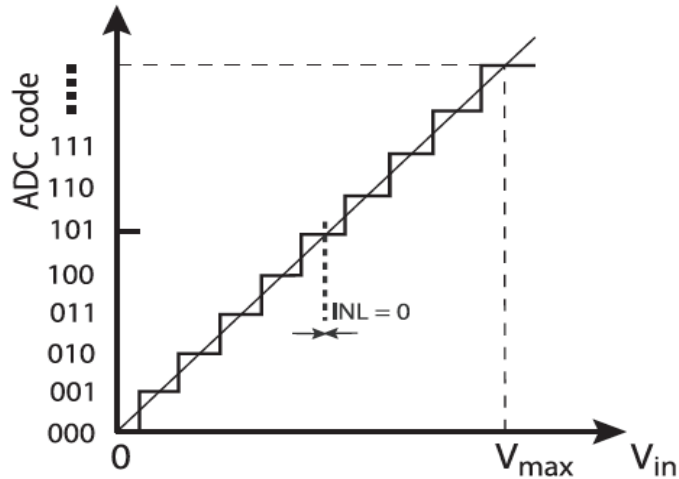
- goal: discriminate at the same fraction, constant in time.
- An inverted and attenuated pulse is superimposed on the delayed pulse.
- Note time-stable zero-crossing point.



$$v_{sum}(t) = v_{in}(t - t_d) - kv_{in}(t)$$

(Elements of ...) Digitisation





$$1 \text{ LSB} \hat{=} \frac{V_{max} - V_{min}}{2^n - 1}$$

quantization error $\delta = \frac{\text{LSB}}{\sqrt{12}}$

$$\text{SNR} = \text{full input range} / \delta$$

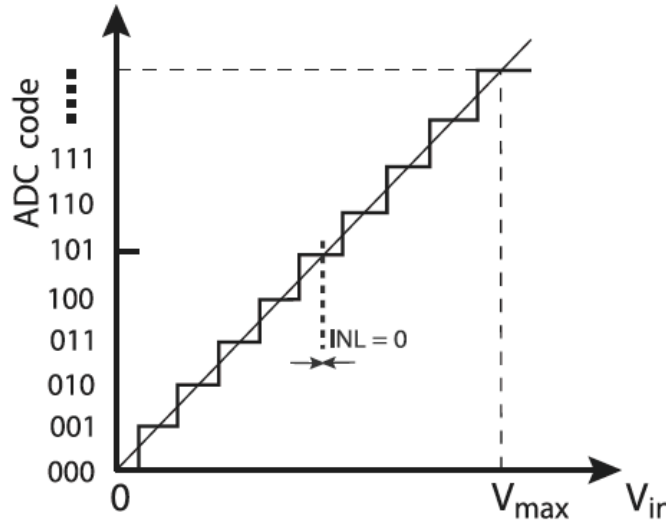
$$= 20 \log_{10} (2^n \sqrt{12}) \approx (6.02 n + 10.8) \text{ dB}$$

(n = no. of bits)

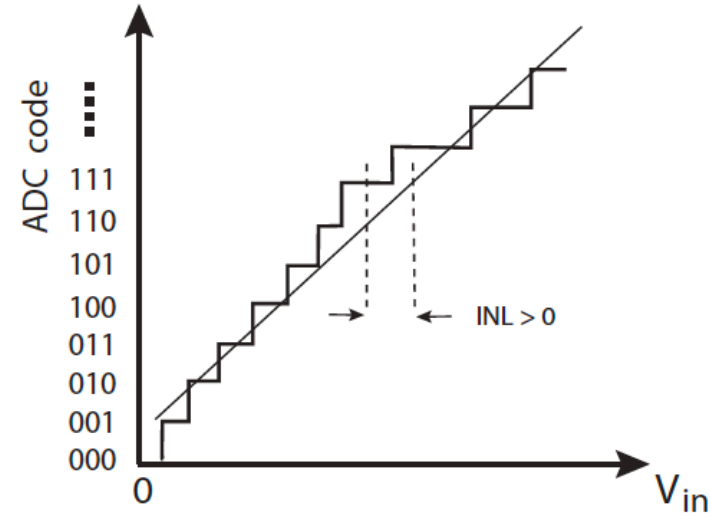
What matters?

- **Resolution:** precision of the code;
- **INL (integral non-linearity):** proportionality of output to input;
- **DNL (differential non-linearity):** homogeneity of digitisation steps;
- **Conversion speed**
- **Rate capability:** how fast successive signals can still can be correctly digitised
- **Stability:** sensitivity of conversion quality with wrt. to time, temperature, other params

quantization error
 zero-point error
 slope error
linearity errors



(a) Perfectly linear ADC.



(b) Integral non-linearity.

INL describes the total deviation from the expected linear behaviour.

INL = maximum deviation of the measured midpoints from ideal line

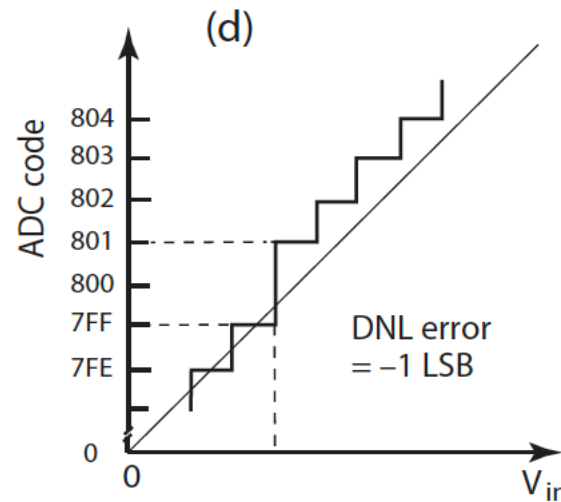
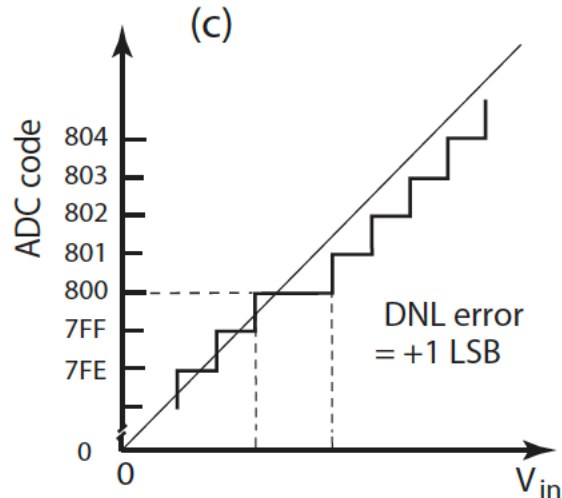
given as fraction of V_{\max} or (usually) in units of the voltage step which corresponds to the lowest-valued bit (LSB units).

DNL = measure of the homogeneity of subsequent digitisations

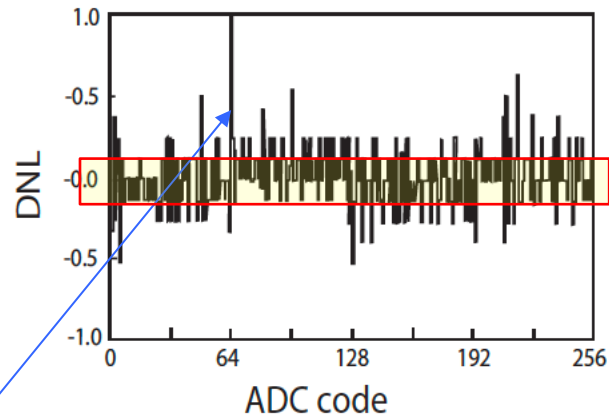
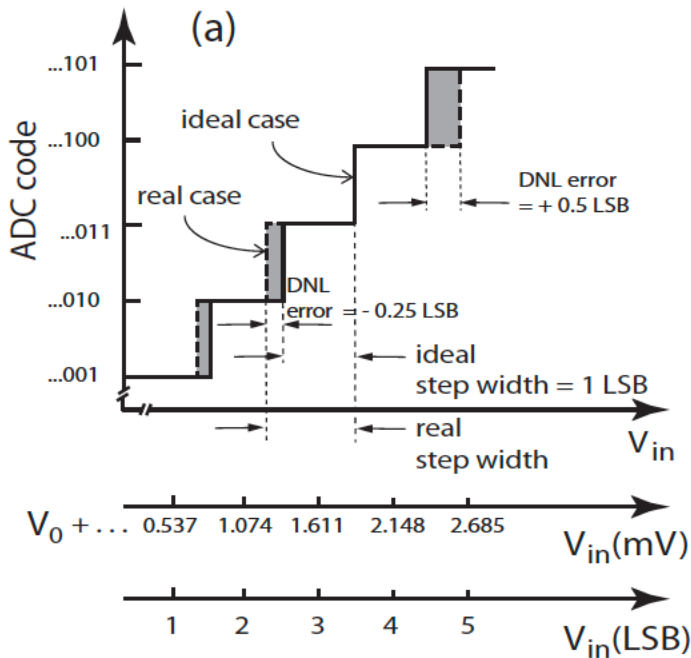
The midpoints of the voltages of subsequent codes should ideally be separated by exactly 1 LSB. The DNL describes local relative deviations of ADC codings from the (ideal) step width (1 LSB):

$$DNL_i = \frac{V_{i+1} - V_i}{LSB} - 1 \quad \text{for } i = 0, 1, 2, \dots, 2^n - 2$$

specified as a fraction or a multiple of ± 1 LSB.



DNL errors larger than -1 LSB are required to guarantee no 'missing codes'.



measurement: sweep V_{in} linearly and plot DNL_i as a function of the code.

for overall DNL either

$$DNL := \max_i (|DNL_i|)$$

or

$$DNL_{rms} := \left(\frac{1}{2^n - 2} \sum_{i=0}^{2^n - 2} (DNL_i)^2 \right)^{1/2}$$

SAR = Successive Approximation Register

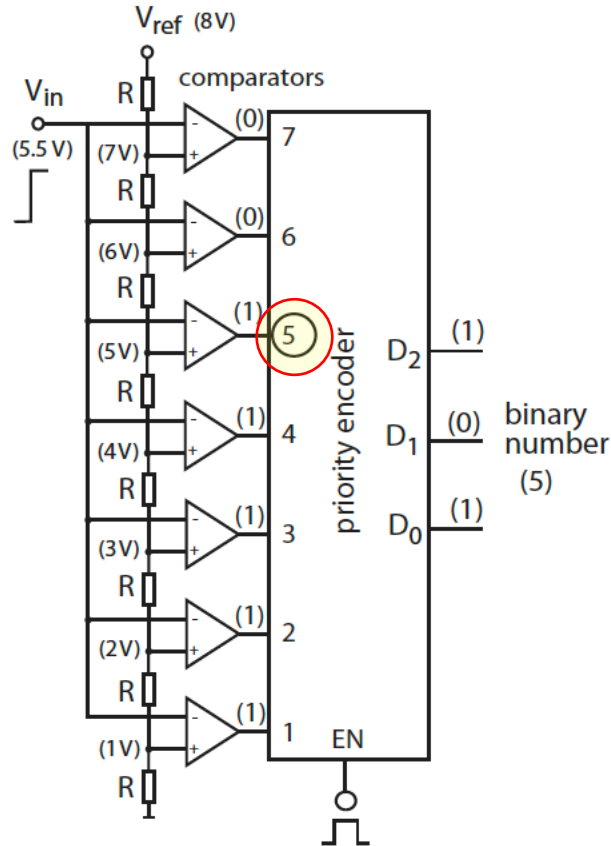
Flash ADC

Wilkinson (→ Dual Slope) ADC

Pipeline ADC

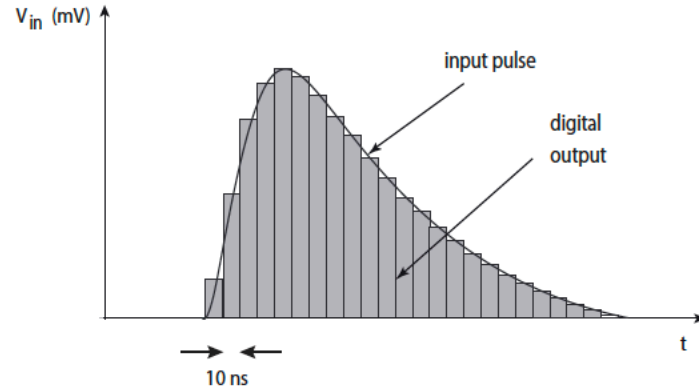
... more

here
3-bit

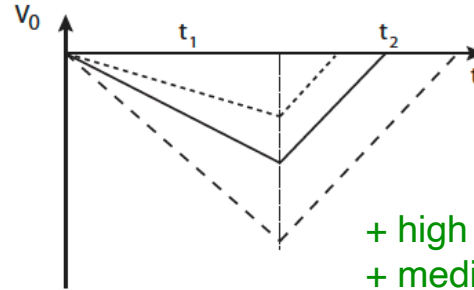
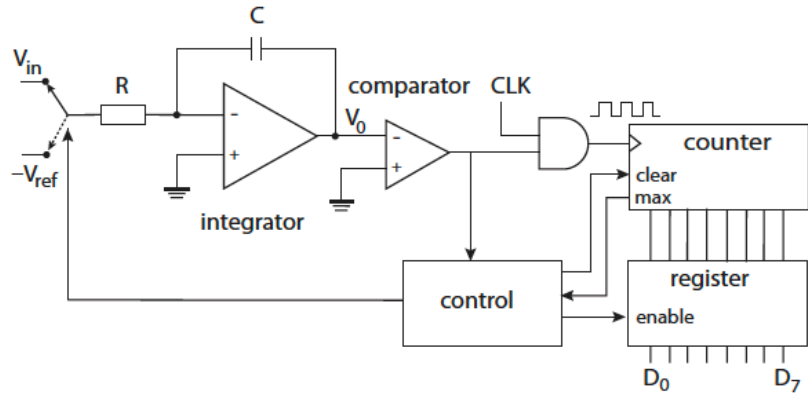


(a) Flash ADC block diagram.

- + fast
- high power cons.
- large chip area needed



(b) Digitisation of a pulse.



- + high resolution
- + medium circuit effort
- + chip area ~independent of resolution
- + independent of fabrication variations
- + good noise immunity
- comparison to other ADCs

- Feedback capacitor is **linearly charged and discharged**, controlled by a counter.
- Charging for a time t_1 , usually until the counter reaches its maximum value determined by V_{in} .
- Then the counter is reset and the **input is switched to $-V_{ref}$** (discharging starts).
- Slope (and time) of **discharge** depends on $-V_{ref}$
- Slope (and time) of **charge** depends on V_{in} .
- Discharging proceeds with constant slope (set by $-V_{ref}$) but with variable duration t_2 until V_0 reaches zero.
- The duration (t_2) depends on the height of V_0 reached after the end of the charging process.
- => **The counter value at t_2 encodes V_{in} and is transferred into the register.**

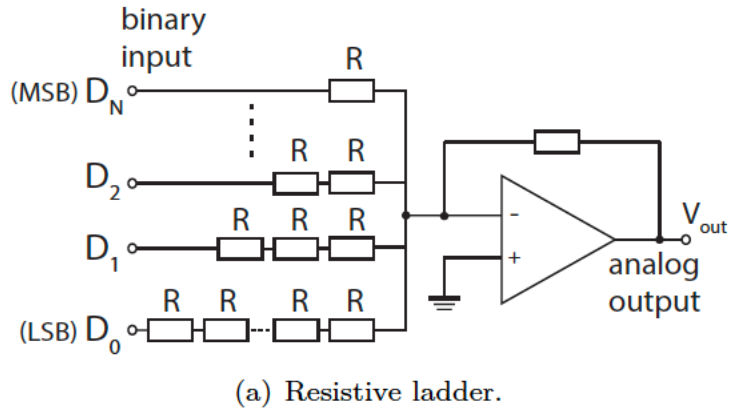
ADC type	Rel. speed (samples per s)	Resolution (bits)	Chip area	Power consumption
SAR	slow–medium ($< 2 \text{ Ms/s}$)	8–16	small	low
Dual-slope	slow ($< 100 \text{ ks/s}$)	12–20	medium	low
Flash	very fast ($< 5 \text{ Gs/s}$)	4–12	large	high
Pipeline	fast ($< 500 \text{ Ms/s}$)	8–16	medium	medium

skip DAC, TDC

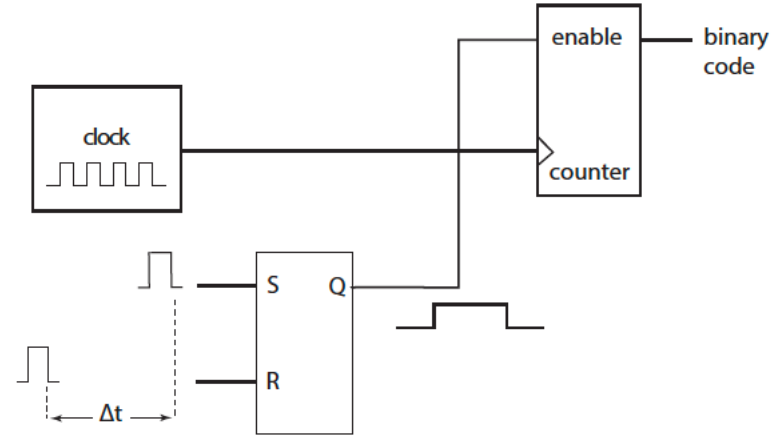


DACs are characterised similarly to ADCs by **resolution**, **linearity**, and **conversion speed**. Integral (INL) and differential (DNL) nonlinearity are also defined as for ADCs

DAC

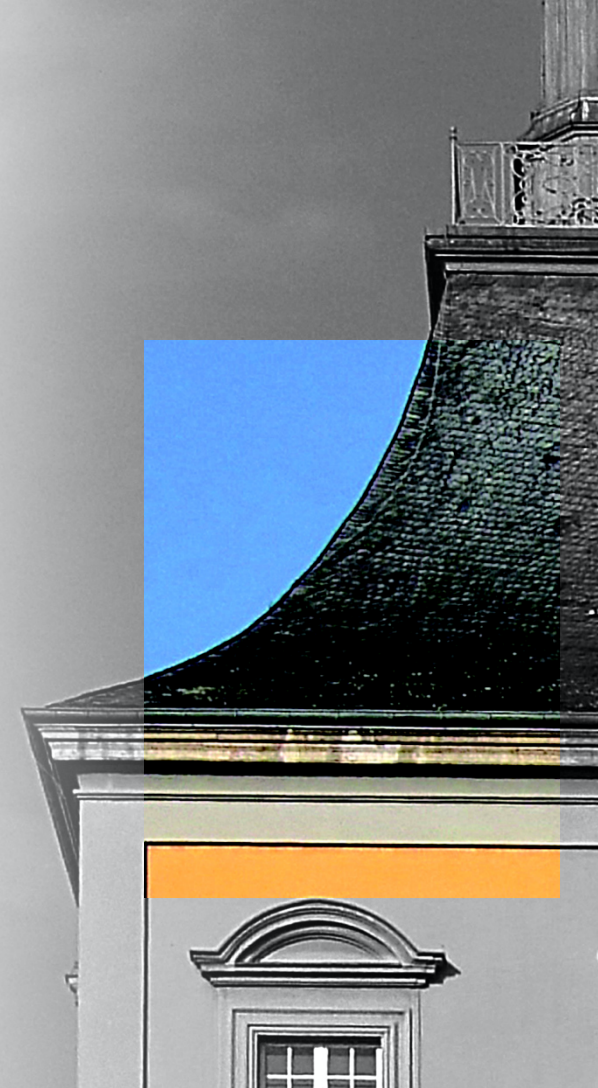


TDC

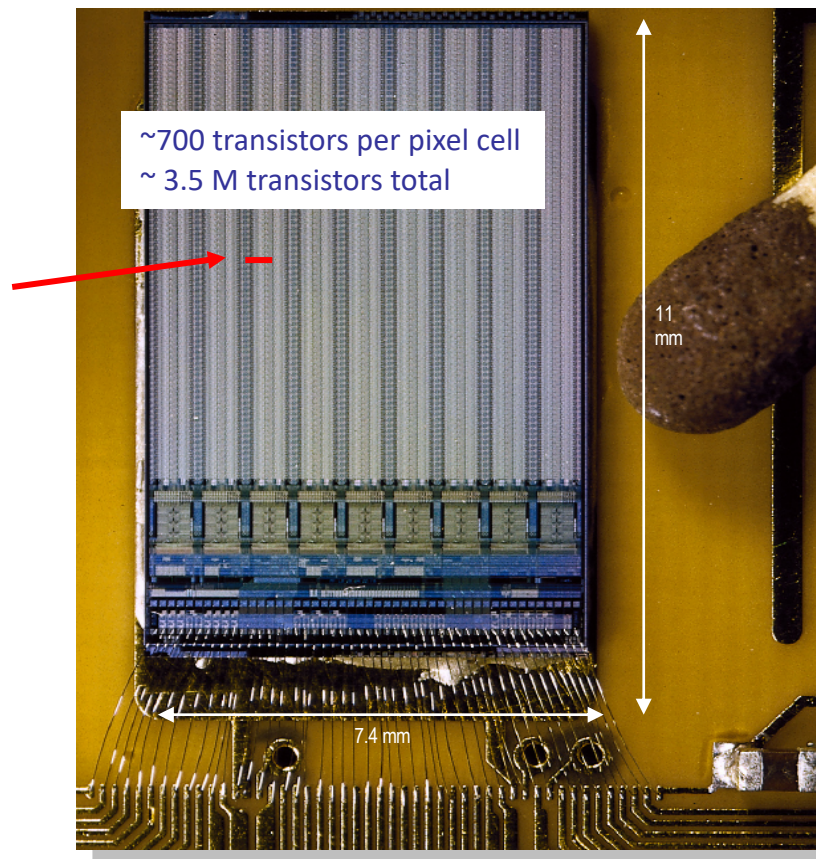


AN EXAMPLE FOR WHAT WE
DISCUSSED SO FAR

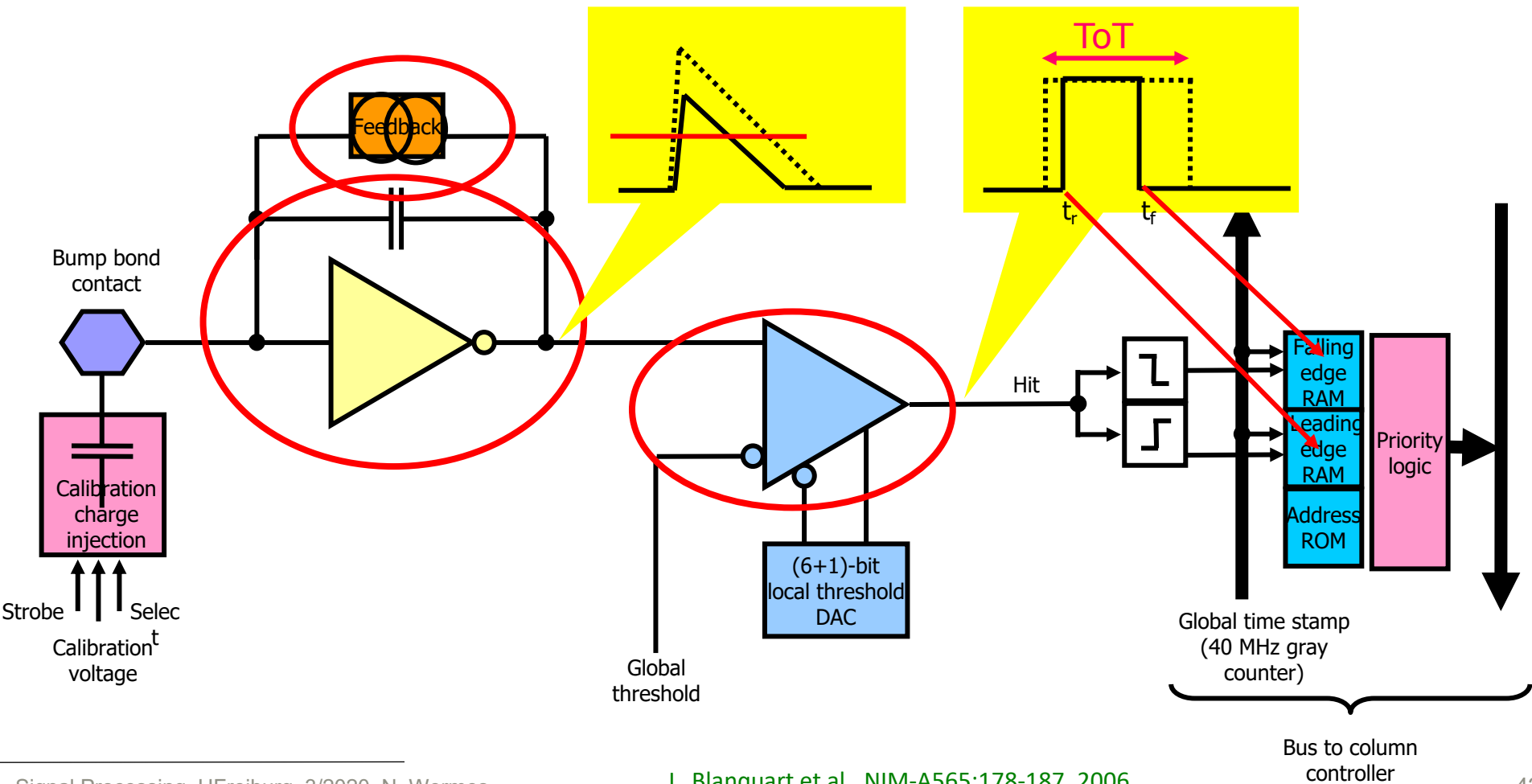
(ATLAS) PIXEL READOUT CHIP



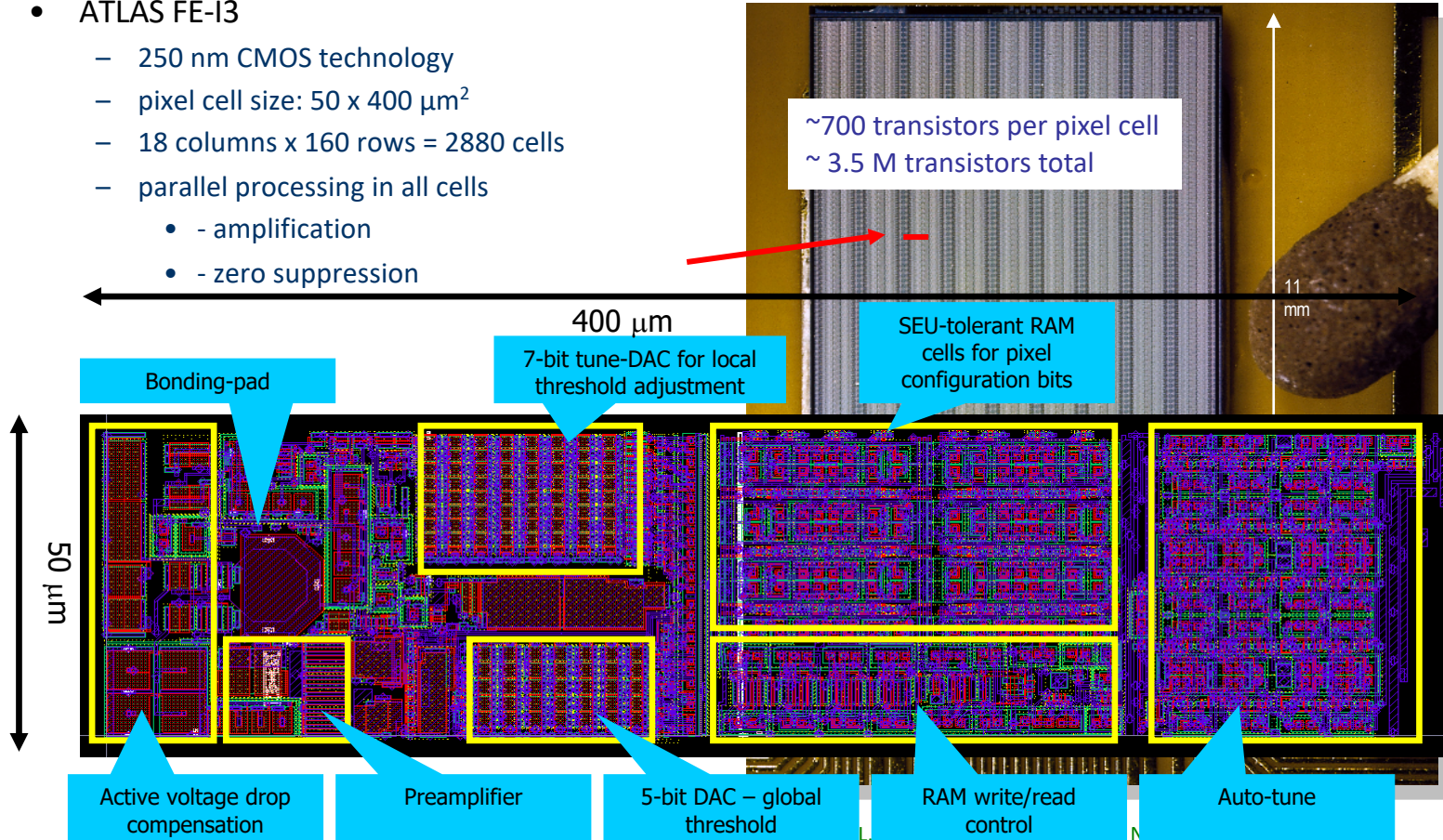
- ATLAS FE chips (FE-I3 and FE-I4)
 - 250 nm (IBL 130 nm) CMOS technology
 - pixel cell size: $50 \times 400 \mu\text{m}^2$
 - 18 columns x 160 rows = 2880 cells
 - parallel processing in all cells
 - - amplification
 - - zero suppression



Pixel cell: amplifier + quasi shaper + discriminator

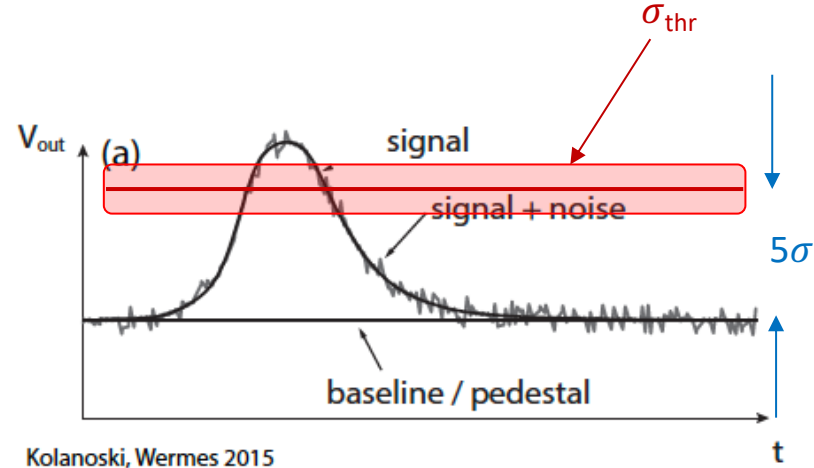
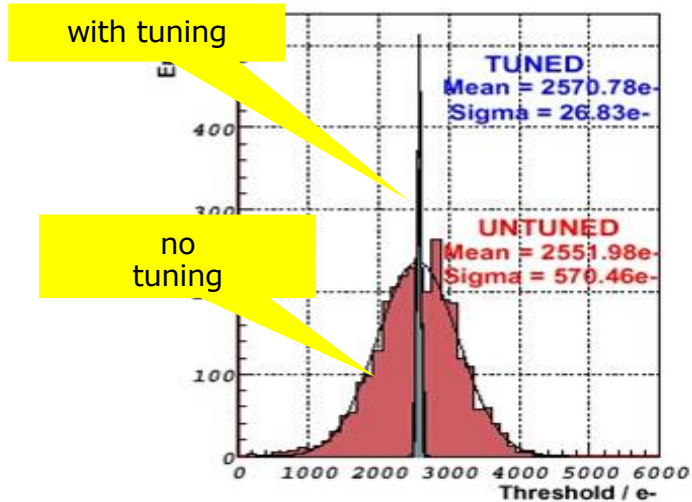


- ATLAS FE-I3
 - 250 nm CMOS technology
 - pixel cell size: $50 \times 400 \mu\text{m}^2$
 - 18 columns x 160 rows = 2880 cells
 - parallel processing in all cells
 - - amplification
 - - zero suppression



- small noise hit rate
- $\sigma_{\text{noise}} \oplus \sigma_{\text{threshold}} <$
- time stamping $<$

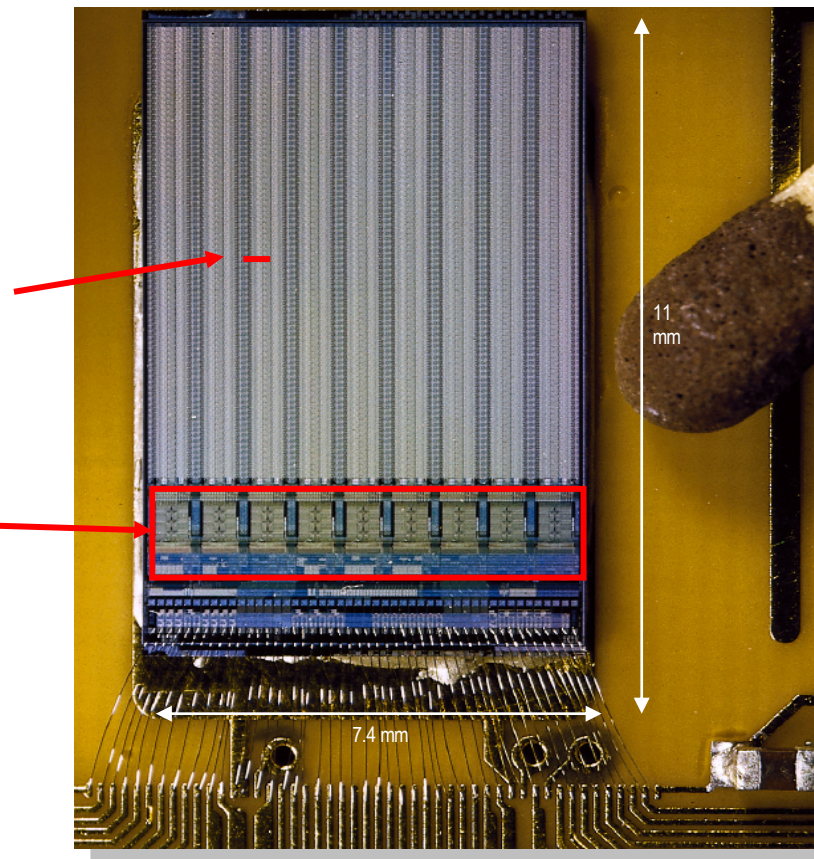
→ low noise and small threshold dispersion
 500 e⁻ @ a threshold of 2500 e⁻
 20 ns after BX for all signal heights



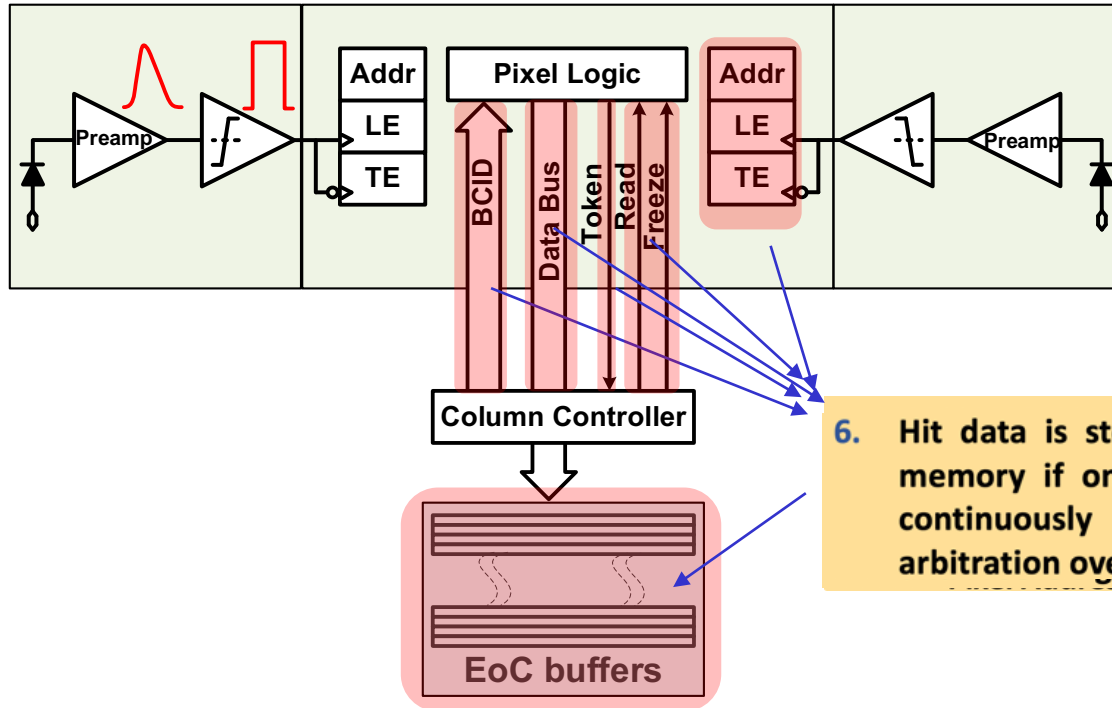
Kolanoski, Wermes 2015

Distribution of pixel cell thresholds

- ATLAS FE-Chip
 - 250 nm CMOS technology
 - pixel cell size: $50 \times 400 \mu\text{m}^2$
 - 18 columns x 160 rows = 2880 cells
 - parallel processing in all cells
 - amplification
 - zero suppression
- end of column logic
 - storage of hit information during trigger latency ($2.5 \mu\text{s}$)
 - hit selection upon L1 trigger



Synchronous readout => time stamping in matrix



- BC ID (40 MHz) distributed in the column

- Hit timing stamped in pixel
- LE: leading edge
- TE: trailing edge
=> Time of arrival: LE
=> Ana. info. from ToT

- Hits read out sequentially, following a token passing scheme on a shared column bus

6. Hit data is stored in the trigger memory if one exists or else is continuously transmitted after arbitration over different columns

- Hits are removed if no trigger coincidence occurs.
- Hit information agreeing with L1 trigger time are read out.

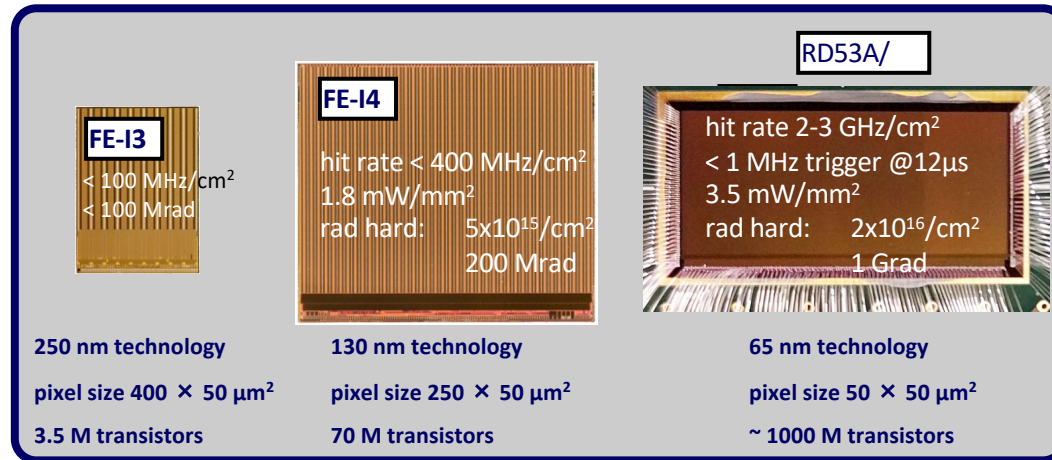
skip upgrades



skip transmission lines

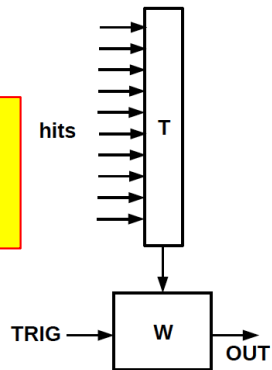


- Effort and costs so large that joint approach (cross experiments) is needed -> **RD53** (20 Institutes)
- Higher hit rate (not smaller pixel size) requires higher logic density -> **65nm TSMC**



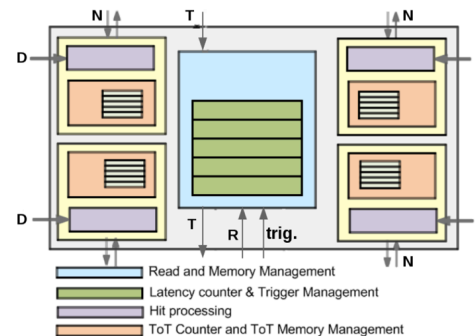
1st generation

- column drain R/O
- FE-I3 like



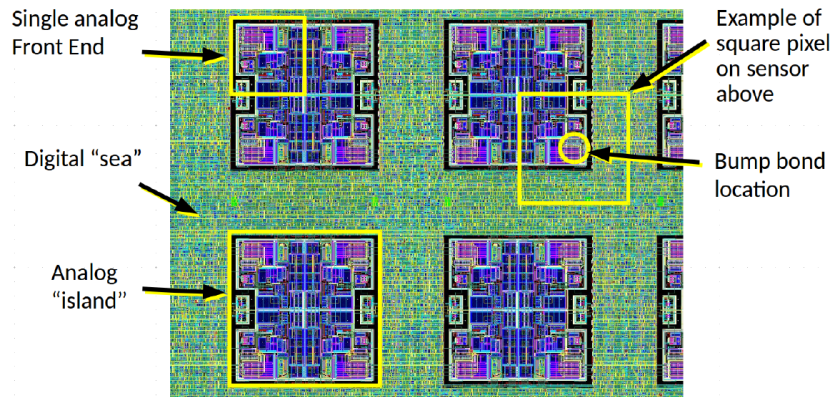
2nd generation

- 4-pixel region logic
- efficient for clusters
- FE-I4 like



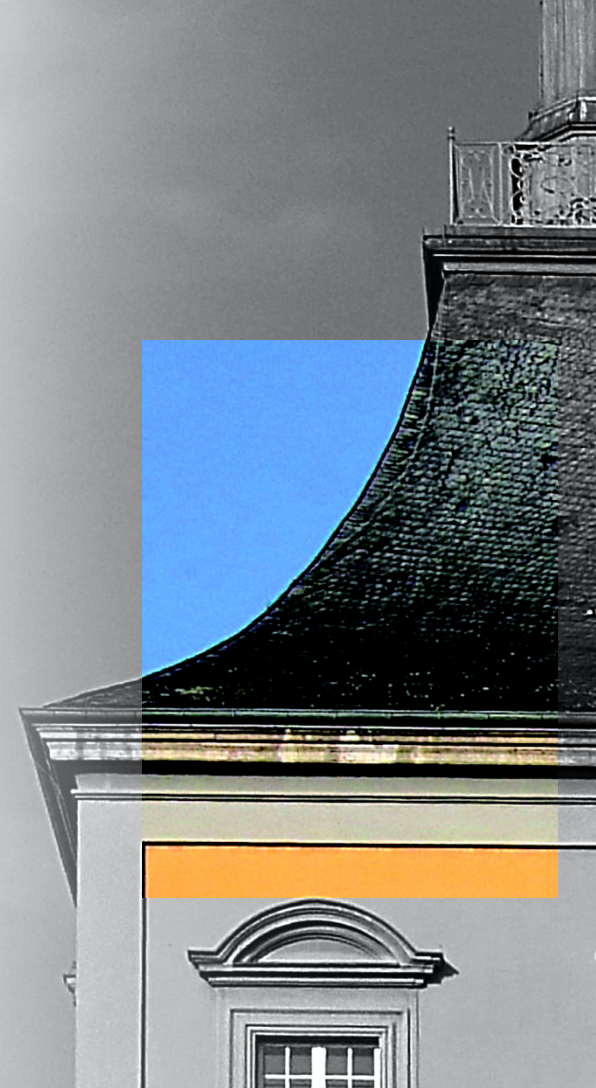
3rd generation

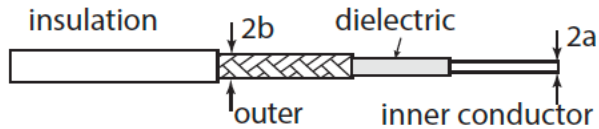
- region architectures with grouped logic -> regional hit draining
- surrounded by synthesized logic ("digital sea")
- RD53 like



"analog islands in digital sea"

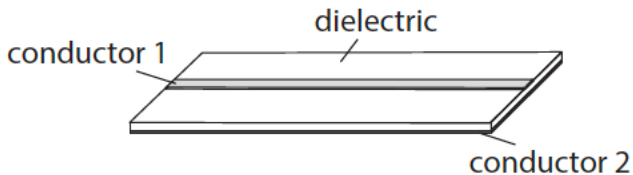
Signal transmission off the detector (transmission lines)





(a) Coaxial cable transmission line.

$$L' \approx \frac{\mu\mu_0}{2\pi} \ln \frac{b}{a} \quad C' \approx \frac{2\pi\epsilon\epsilon_0}{\ln(b/a)}$$



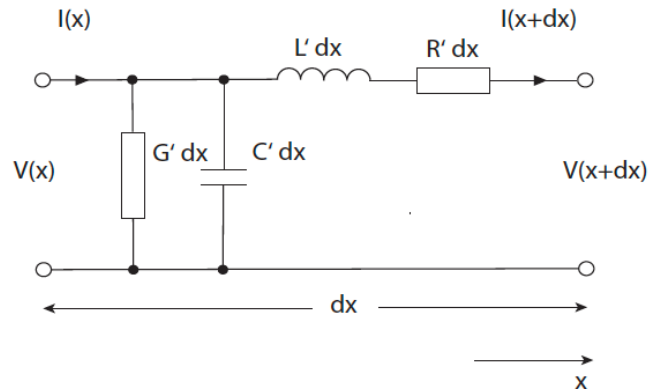
(b) Microstrip line.

solutions = forw. & backw. running waves

$$V(x, t) = V_0 e^{i\omega t - \gamma x} = V_0 e^{i(\omega t \mp \beta x)} e^{\mp \alpha x}$$

damping

equivalent circuit



telegraph (wave) equations

$$\frac{\partial^2 V}{\partial x^2} - L' C' \frac{\partial^2 V}{\partial t^2} = (L' G' + R' C') \frac{\partial V}{\partial t} + R' G' V$$

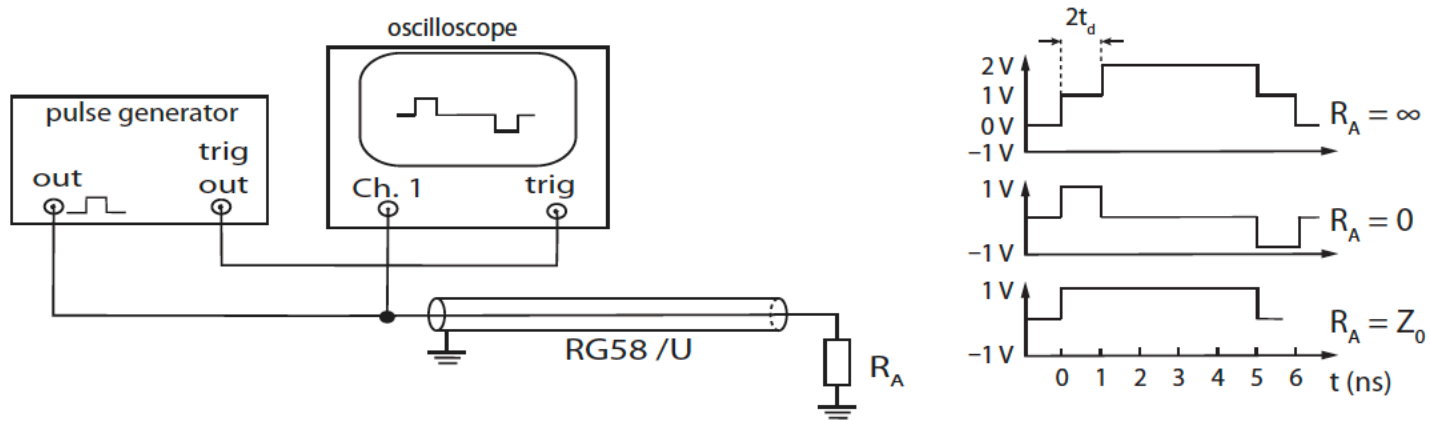
$$\frac{\partial^2 I}{\partial x^2} - L' C' \frac{\partial^2 I}{\partial t^2} = (L' G' + R' C') \frac{\partial I}{\partial t} + R' G' I,$$

$$c_{ph} = \frac{1}{\sqrt{L' C'}} = \frac{1}{\sqrt{\epsilon\epsilon_0 \mu\mu_0}}$$

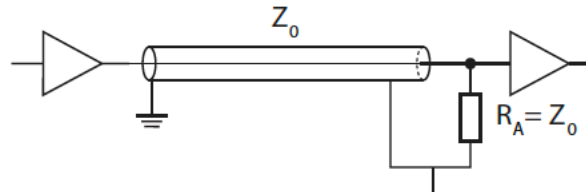
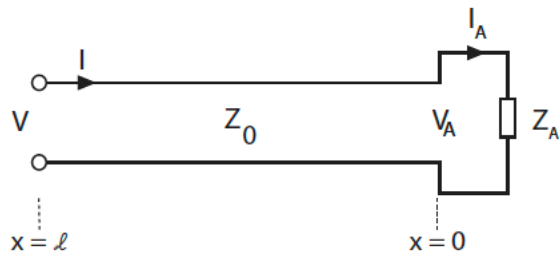
propagation velocity

$$Z_0 = \frac{V}{I} = \sqrt{\frac{L'}{C'}}$$

wave impedance of transmission line



Termination schemes



standard
(receiving-end termination)

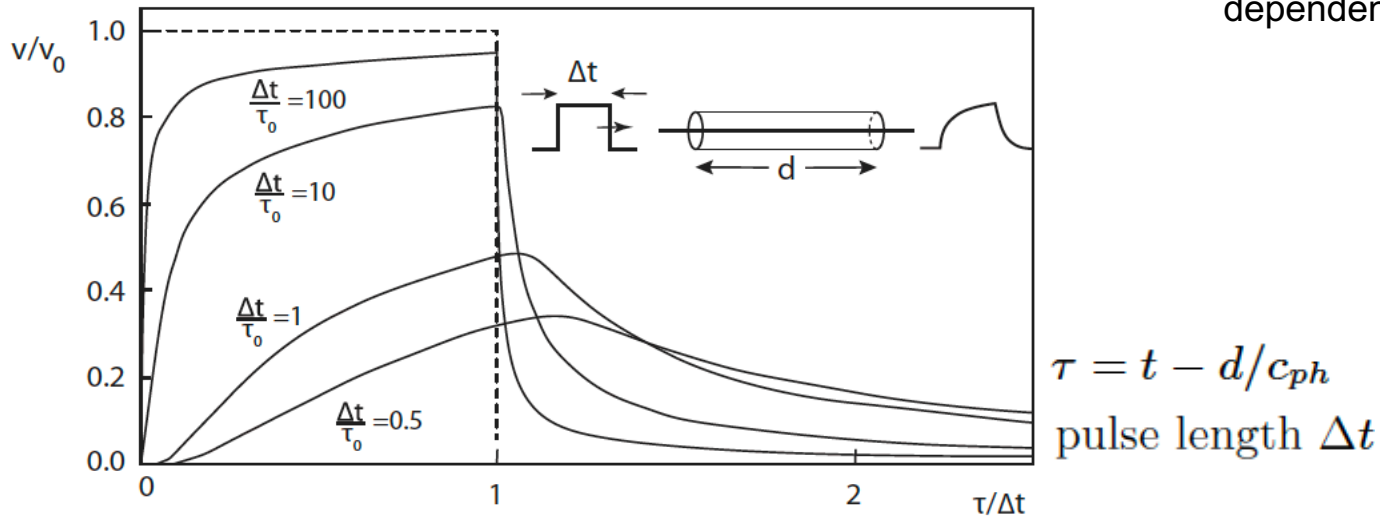
(additional) sending-end
termination

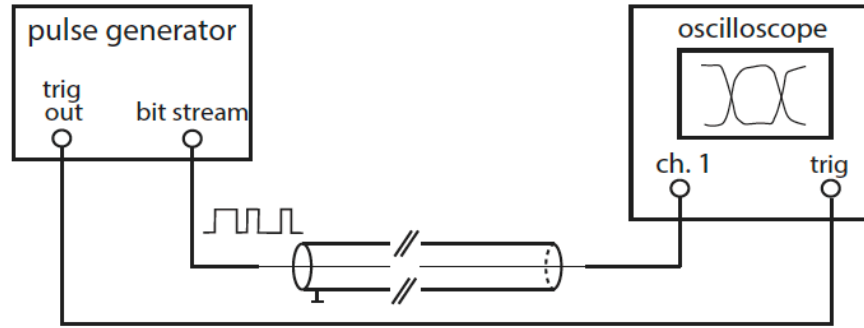
however: 50% reduction of
signal from left.

note: \triangleleft - have $Z_{in} = \text{high}$, $Z_{out} = \text{low}$

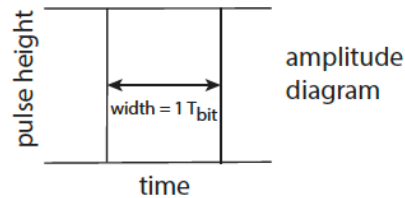
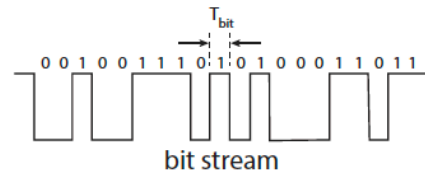
$$V(x, t) = V_0 e^{i\omega t - \gamma x} = V_0 e^{i(\omega t \mp \beta x)} e^{\mp \alpha x} \quad \Rightarrow \quad v(t) = v_0 \operatorname{erfc} \left(\frac{1}{2\sqrt{\tau/\tau_0}} \right)$$

τ_0 = cable-characteristic, frequency-dependent rise time function





(a) Measurement set-up.

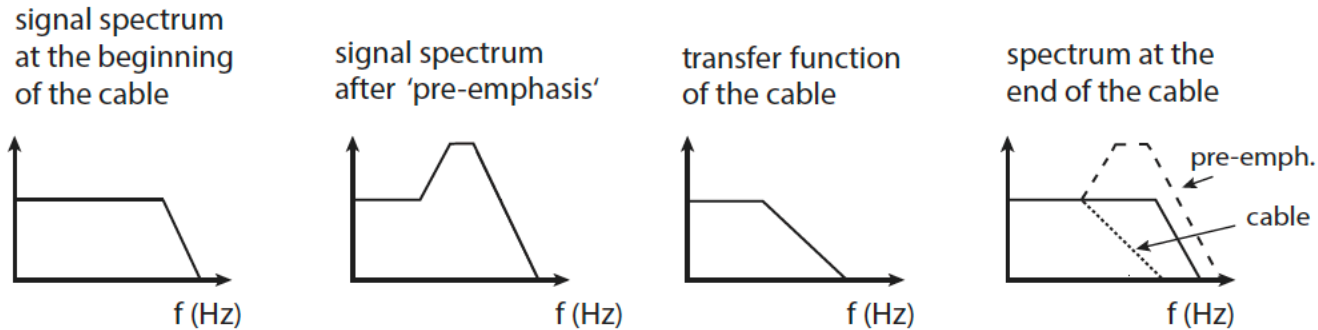


(b) Ideal transmission.

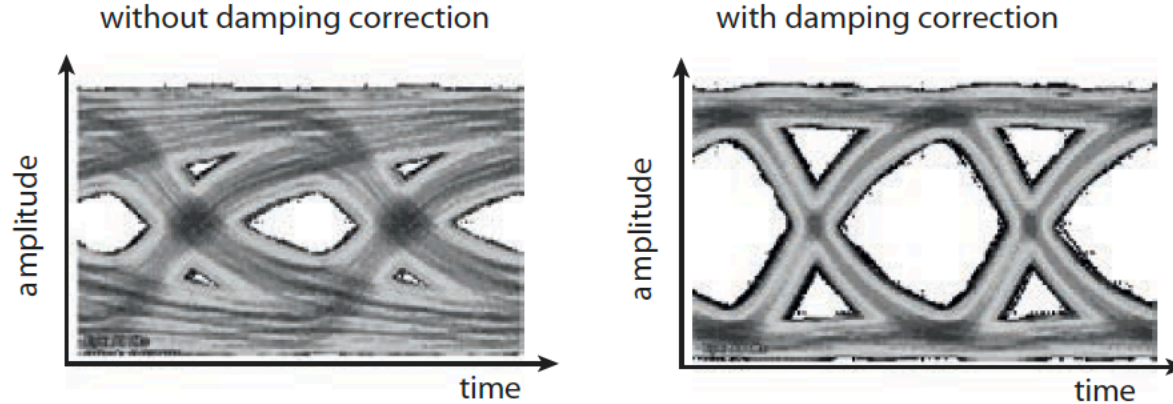


(c) Real transmission.

Kolanoski, Wermes 2015

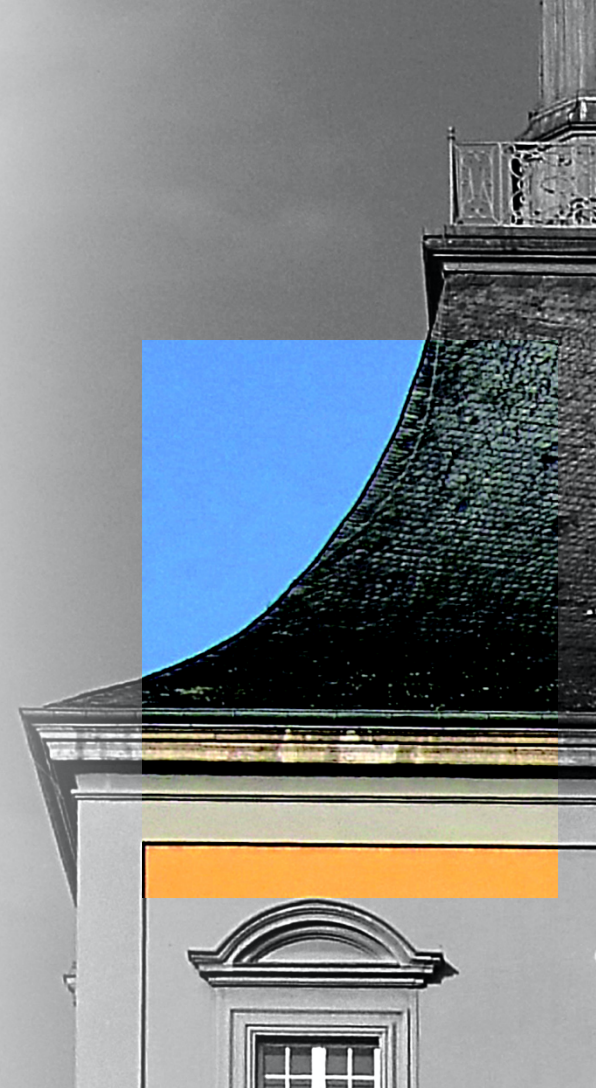


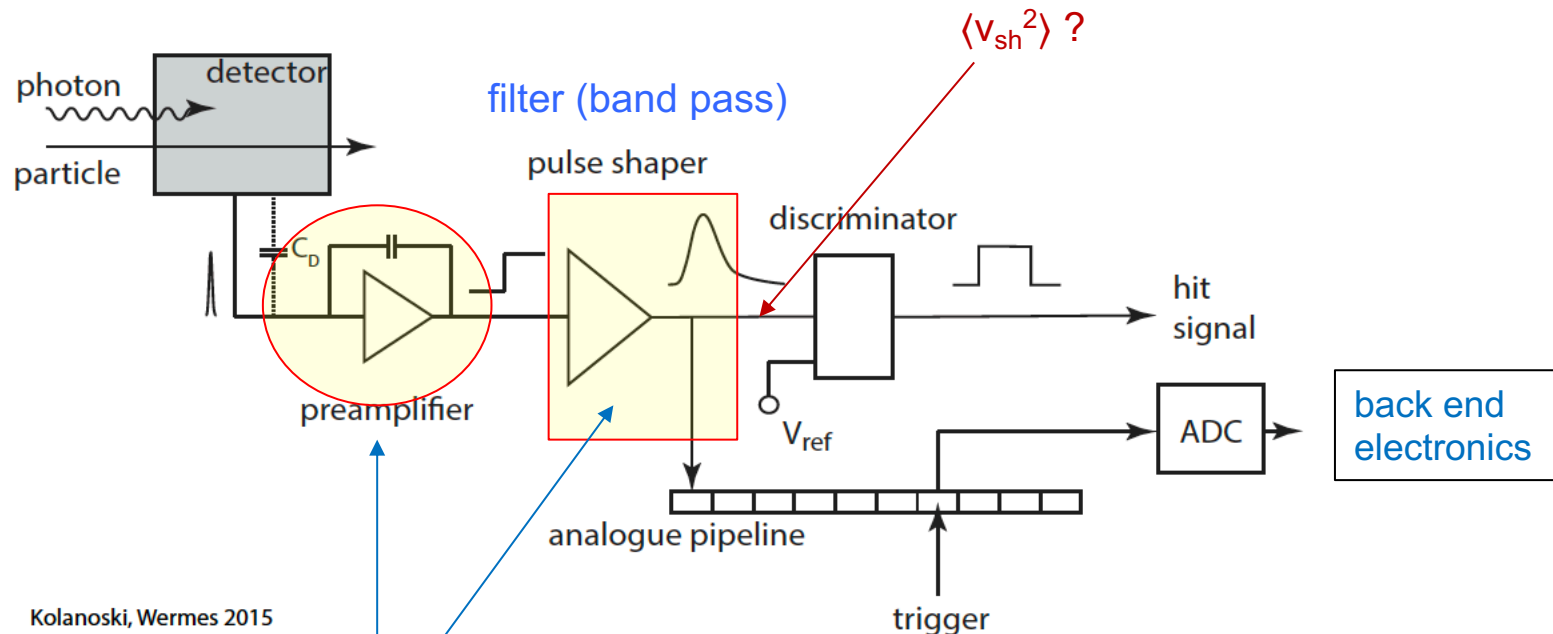
(a) Damping correction by means of *pre-emphasis*-filter (double logarithmic representation).



(b) Eye diagram without (left) and with (right) correction.

Noise of a readout system

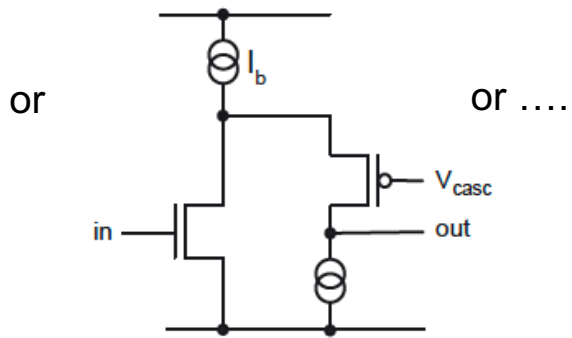
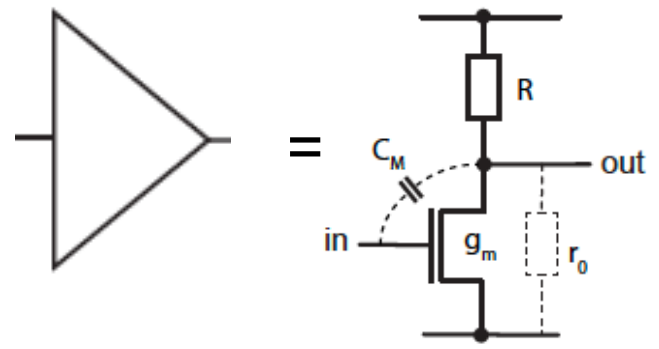




Kolanoski, Wermes 2015

the dominant noise of a system is hidden in these parts

Most critical wrt noise: the (pre)amplifier



metall
polysilicon
oxid
n+ implant
p- substrat

Dimensionierung der Transistoren

$\Delta V_{GS} = 1V$

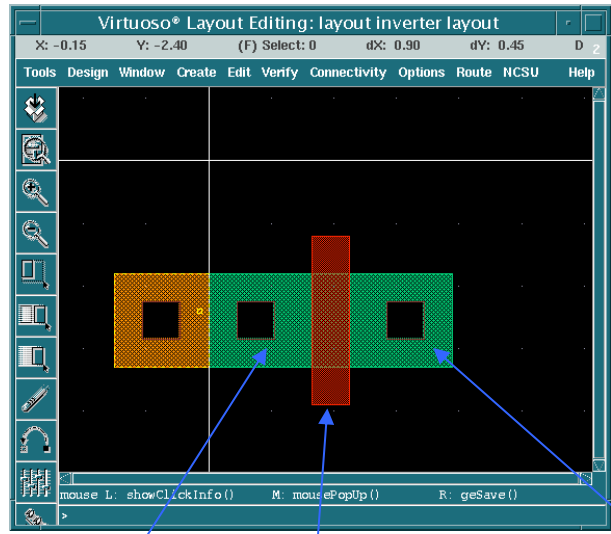
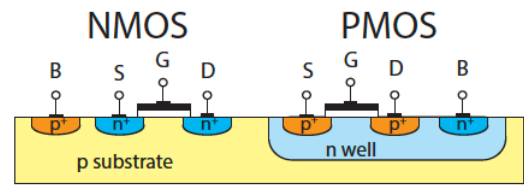
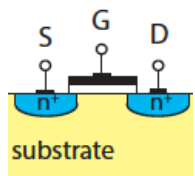
W/L groß
hohe "Verstärkung"

$\Delta V_{GS} = 1V$

W/L klein
hoher Ausgangswiderstand

Layout: nMOS and pMOS

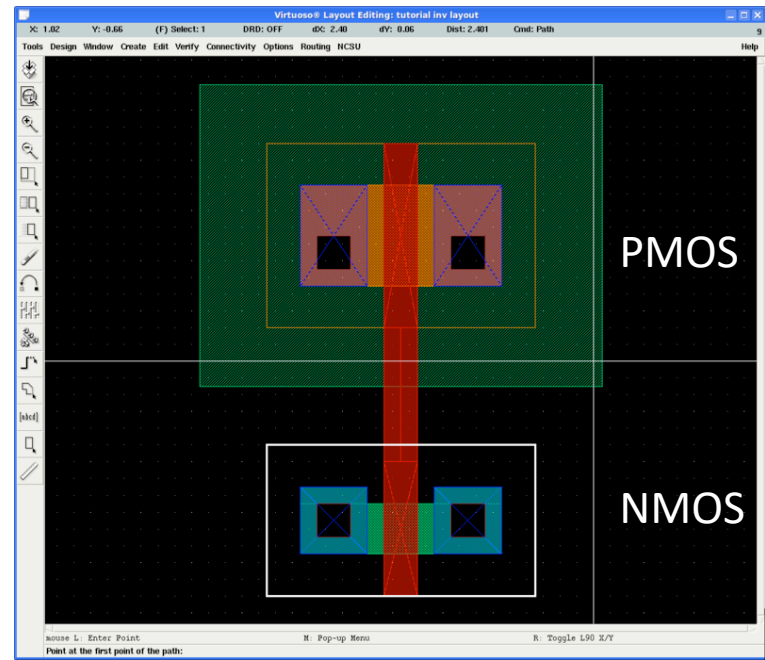
MOS transistor



Source

Gate (area = $W \times L$)

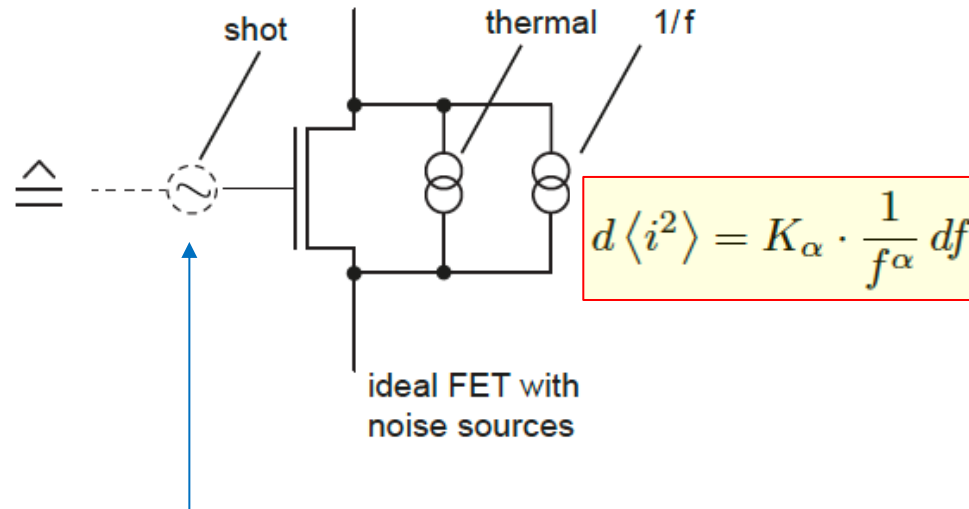
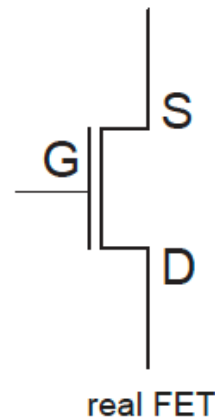
Drain



PMOS

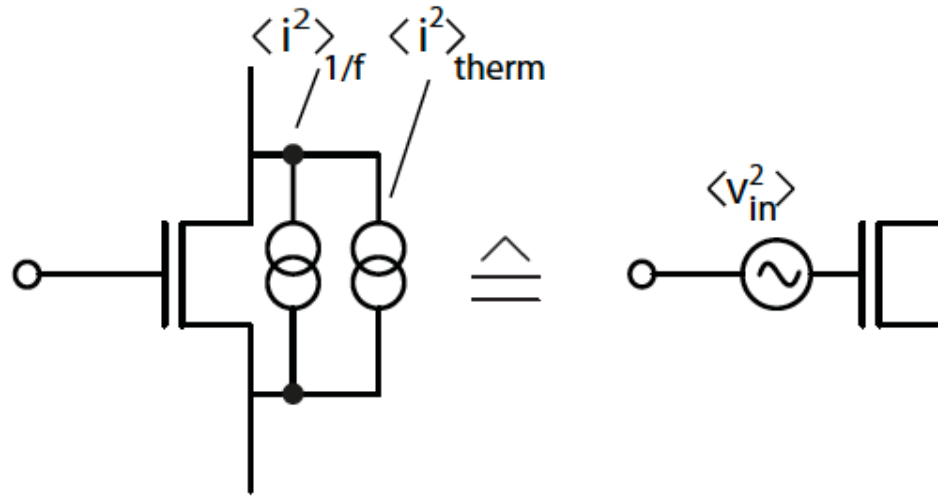
NMOS

$$\frac{d\langle i^2 \rangle_{\text{therm}}}{df} = \frac{4kT}{R} df \rightarrow \frac{4kT}{\frac{1}{2/3g_m}} = 4kT \frac{3}{2} g_m$$



if shot noise input exists
(e.g. from leakage current of a Si detector)

“parallel current noise can be described by serial voltage noise”



$$\langle i_D^2 \rangle = \langle (g_m v_{\text{in}})^2 \rangle$$

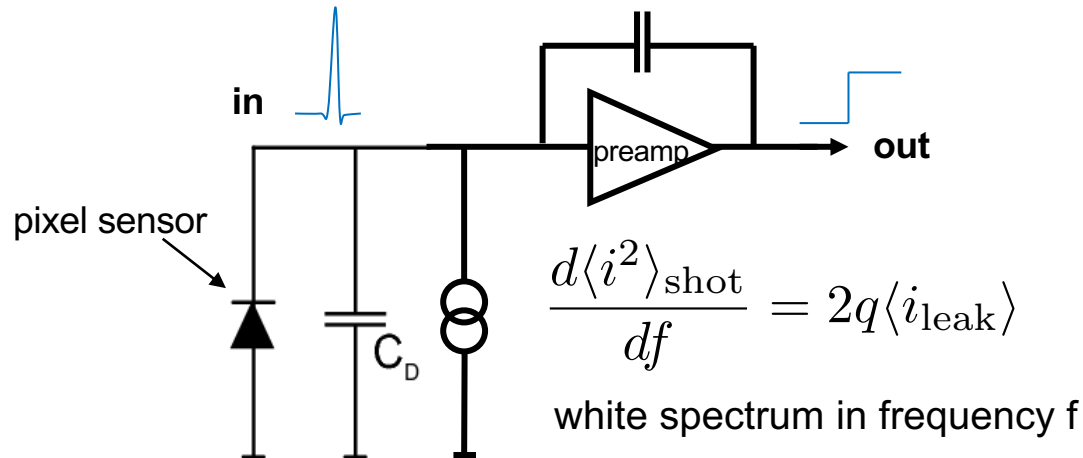
$$g_m = \partial I_D / \partial V_{GS} \propto \sqrt{I_D} \propto \sqrt{W/L}$$

(in saturation)

three physical noise sources:

- number fluctuations of quanta → 1. shot noise and 2. 1/f noise
- velocity fluctuations of quanta → 3. thermal noise

where do they appear in a typical pixel detector readout chain ?



three physical noise sources:

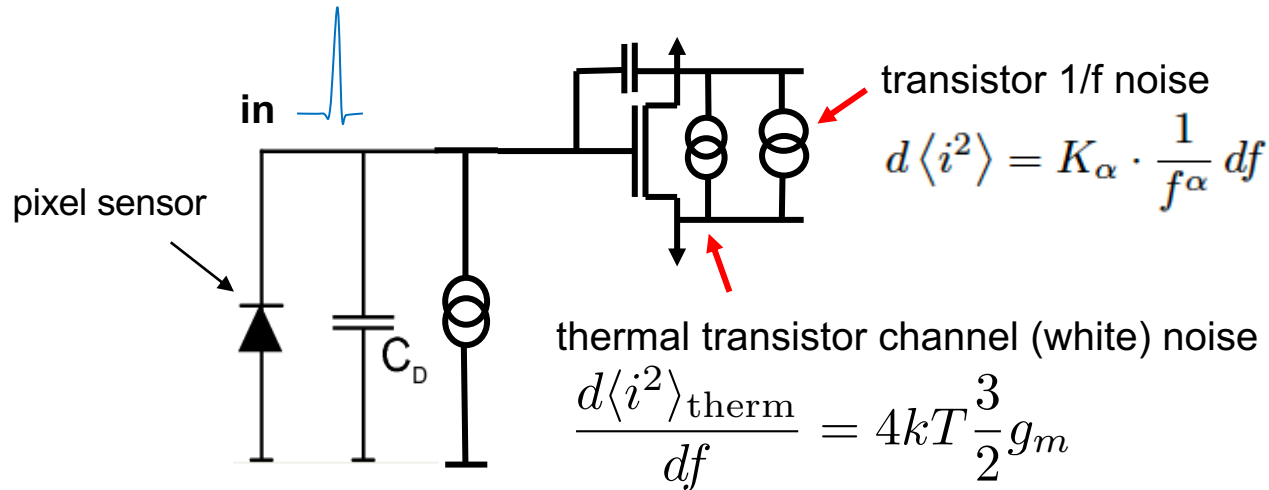
number fluctuations of quanta →

velocity fluctuations of quanta →

1. shot noise and 2. 1/f noise

3. thermal noise

where do they appear in a typical pixel detector readout chain ?

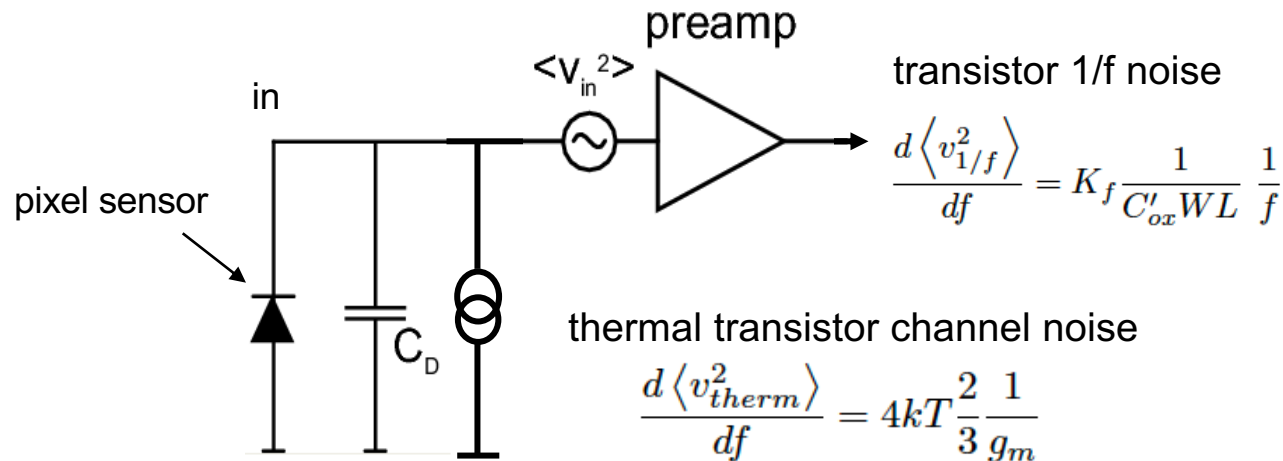


three physical noise sources:

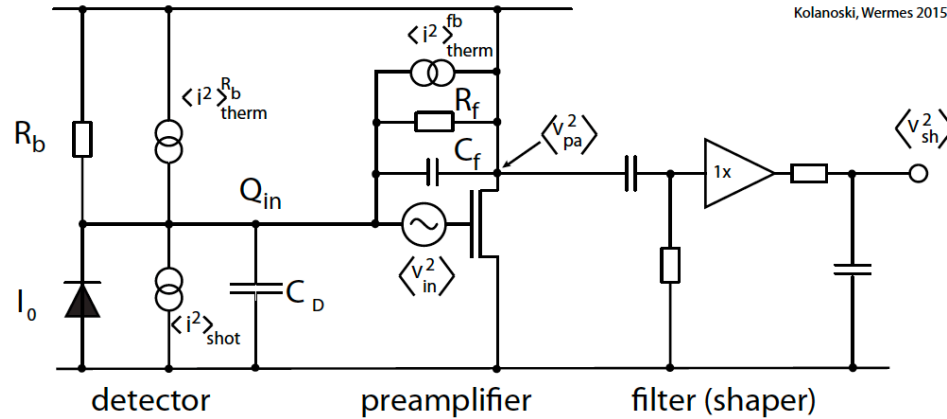
number fluctuations of quanta →
velocity fluctuations of quanta →

1. shot noise and 2. 1/f noise
3. thermal noise

where do they appear in a typical pixel detector readout chain ?

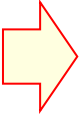


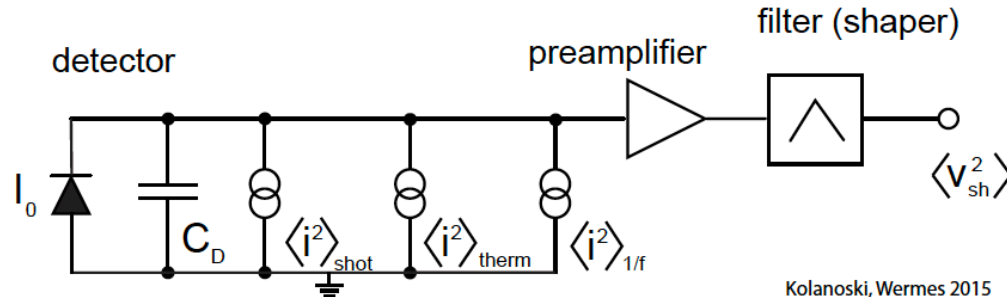
the situation discussed so far ...



It is useful to treat the **serial voltage noise sources** (1/f and thermal noise) as **equivalent parallel current noise** via the capacitance C_D at the input of the preamplifier. This is possible via the relationship

$$\langle i_{in}^2 \rangle \approx \langle v_{in}^2 \rangle (\omega C_D)^2 \quad (\text{with } \omega = 2\pi f)$$


equivalent circuit

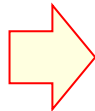


Kolanoski, Wermes 2015

$$\frac{d\langle i_{in}^2 \rangle}{d\omega} = \underbrace{2eI_0 \frac{1}{2\pi}}_{\text{'shot'}} + \underbrace{\frac{K_f}{C_{ox}WL} \frac{1}{f} (\omega C_D)^2}_{\text{'1/f'}} + \underbrace{\frac{4kT}{g_m} \frac{2}{3} (\omega C_D)^2}_{\text{'thermal'}}$$

This noise current, flowing through the feedback capacitance C_f , generates a noise voltage behind the preamplifier:

$$\langle v_{pa}^2 \rangle = \langle i_{in}^2 \rangle \left(\frac{1}{\omega C_f} \right)^2$$



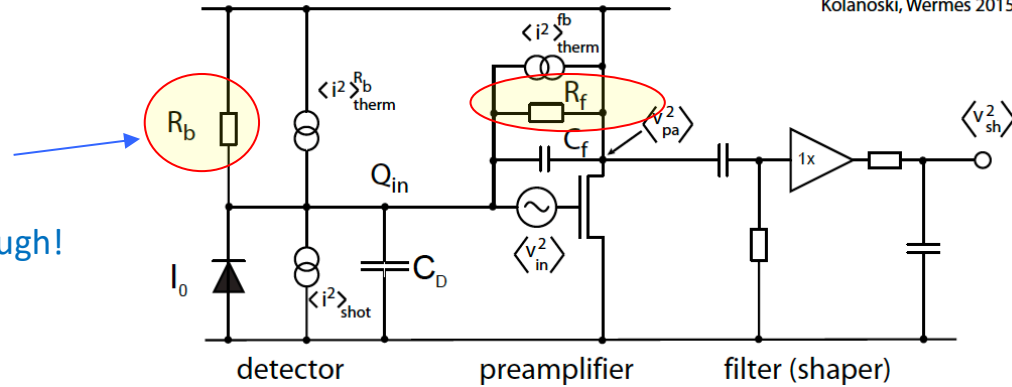
$$\begin{aligned} \frac{d\langle v_{pa}^2 \rangle}{d\omega} &= \frac{eI_0}{\pi\omega^2 C_f^2} + K_f \frac{1}{C_{ox}WL} \frac{C_D^2}{C_f^2} \frac{1}{\omega} + \frac{4}{3\pi} \frac{kT}{g_m} \frac{C_D^2}{C_f^2} \\ &= \sum_{k=-2}^0 c_K \omega^k \end{aligned}$$

$$c_{-2} = \frac{e}{\pi} I_0 \frac{1}{C_f^2}, \quad c_{-1} = K_f \frac{1}{C_{ox}WL} \frac{C_D^2}{C_f^2}, \quad c_0 = \frac{4}{3\pi} kT \frac{1}{g_m} \frac{C_D^2}{C_f^2}$$

Kolanoski, Wermes 2015

$$\frac{d\langle i^2 \rangle_{\text{therm}}}{df} = \frac{4kT}{R} df$$

=> choose R_f large enough!

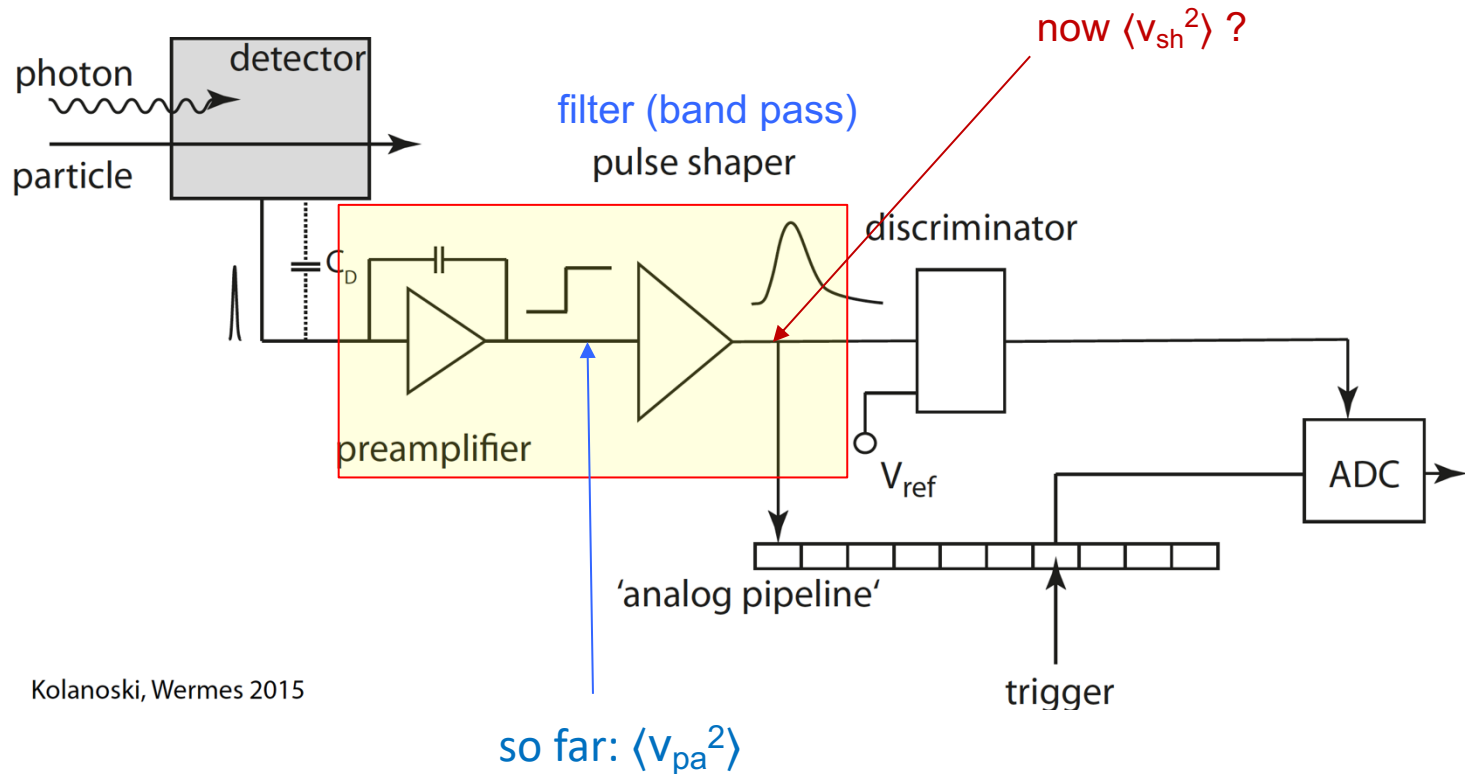


Is/was argued to be small ...

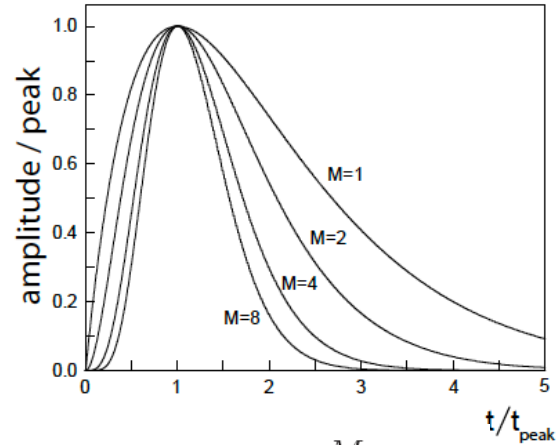
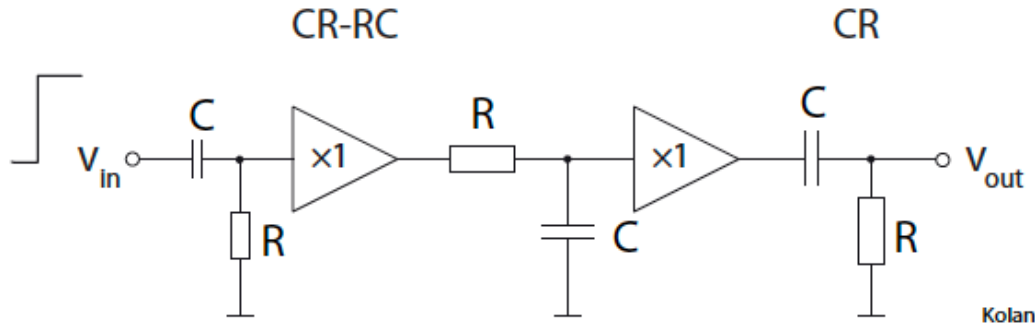
it acts on the preamplifier input in a very similar way as the leakage current shot noise contribution, i.e.

$$\frac{d\langle v_{\text{pa}}^2 \rangle}{d\omega} = \frac{eI_0}{\pi\omega^2 C_f^2} \quad \xrightarrow{2eI_0 \rightarrow \frac{4kT}{R_f}} \quad \frac{d\langle v_{\text{pa}}^2 \rangle_{R_f}}{d\omega} = \frac{2kT}{R_f} \frac{1}{\pi\omega^2 C_f^2}$$

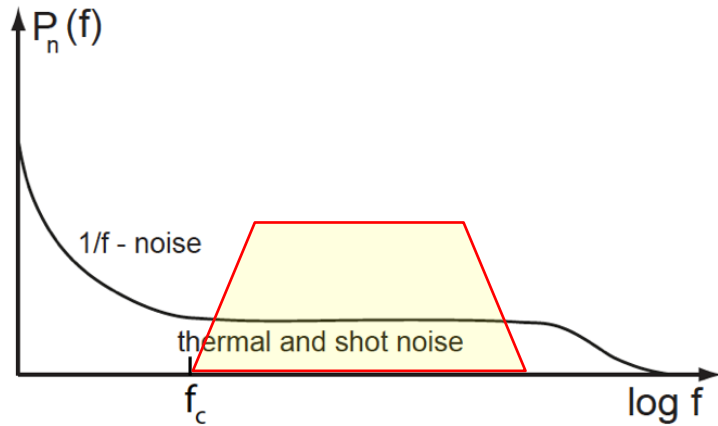
Its magnitude is usually **small** in comparison to the other contributions, in particular to the leakage-current-induced shot noise.



Kolanoski, Wermes 2015

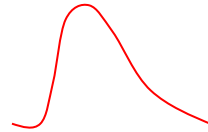


$$f^{(1,M)}(t) = \frac{1}{M!} \left(\frac{t}{\tau} \right)^M e^{-t/\tau}$$



consequences for noise
 BW limitation => lower noise
 on the expense of speed

in the time domain



$$v_{sh}(t) = A \frac{t}{\tau} e^{-\frac{t}{\tau}}$$

peaks at τ with height $A/2.71$

in the frequency domain

$$1/s$$

$$|H(\omega)|^2 = A^2 \left(\frac{\omega\tau}{1 + \omega^2\tau^2} \right)^2 \quad (\text{with } s \rightarrow i\omega)$$

for noise
need square

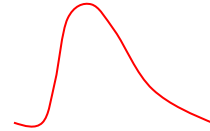
$$\langle v_{sh}^2 \rangle = \int_0^\infty \frac{d\langle v_{pa}^2 \rangle}{d\omega} |H(\omega)|^2 d\omega$$

$$\langle v_{sh}^2 \rangle = \sum_{k=-2}^0 \int_0^\infty c_k \omega^k |H(\omega)|^2 d\omega$$

$$= A^2 \frac{1}{2} \sum_{k=-2}^0 c_k \tau^{-k-1} \Gamma \left(1 + \frac{k+1}{2} \right) \Gamma \left(1 - \frac{k+1}{2} \right)$$

$$\Gamma(x+1) = x\Gamma(x), \quad \Gamma\left(\frac{1}{2}\right) = \sqrt{\pi}, \quad \Gamma(1) = 1$$

in the time domain



$$v_{sh}(t) = A \frac{t}{\tau} e^{-\frac{t}{\tau}}$$

peaks at τ with height $A/2.71$

in the frequency domain

$$1/s$$

$$|H(\omega)|^2 = A^2 \left(\frac{\omega\tau}{1 + \omega^2\tau^2} \right)^2 \quad (\text{with } s \rightarrow i\omega)$$

$$\langle v_{sh}^2 \rangle = \frac{\pi}{4} A^2 \left(c_{-2} \tau + \frac{2}{\pi} c_{-1} + c_0 \frac{1}{\tau} \right)$$

with

$$c_{-2} = \frac{e}{\pi} I_0 \frac{1}{C_f^2}, \quad c_{-1} = K_f \frac{1}{C'_{ox} WL} \frac{C_D^2}{C_f^2}, \quad c_0 = \frac{4}{3\pi} kT \frac{1}{g_m} \frac{C_D^2}{C_f^2}$$

$$\text{ENC} = \frac{\text{noise output voltage (V)}}{\text{output voltage of a signal of } 1 \text{ e}^- \text{ (V/e}^- \text{)}}$$

$$\text{ENC}^2 = \frac{\langle v_{\text{sh}}^2 \rangle}{v_{\text{sig}}^2}$$

for 1e at the input we get

$$v_{\text{sig}} = \frac{A}{2.71} \frac{e}{C_f}$$

↑
peak of shaper pulse

⇒ $\text{ENC}^2 = \frac{\langle v_{\text{sh}}^2 \rangle}{v_{\text{sig}}^2}$

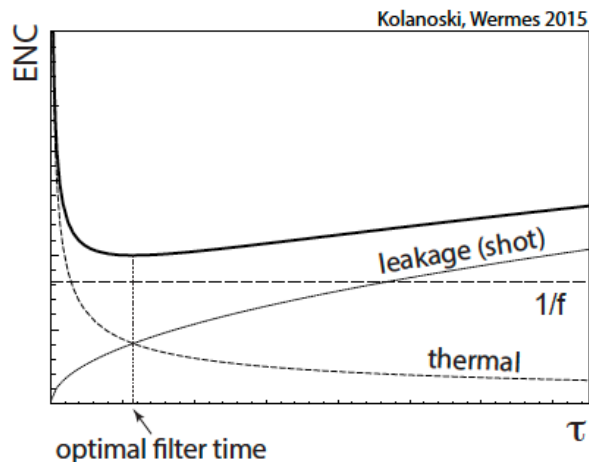
$$\text{ENC}^2(e^{-2}) = \frac{(2.71)^2}{4e^2} \left(eI_0\tau + 2C_D^2 K_f \frac{1}{C'_{ox}WL} + \frac{4kT}{3} \frac{C_D^2}{g_m \tau} \right)$$

$$\text{ENC}^2 = a_{\text{shot}} \tau + a_{1/f} C_D^2 + a_{\text{therm}} \frac{C_D^2}{\tau}$$

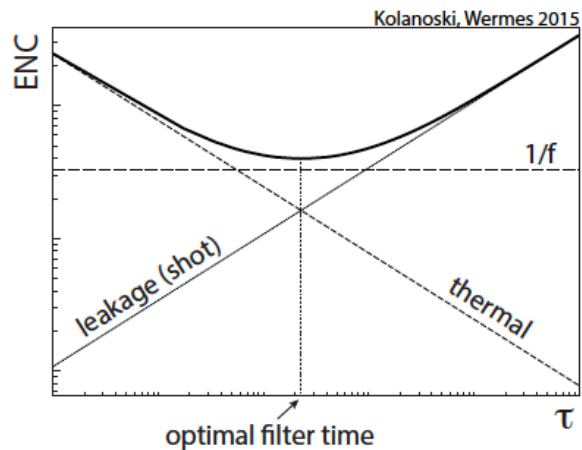
$$\frac{\text{ENC}^2}{e^2} = 11 \frac{I_0}{\text{nA}} \frac{\tau}{\text{ns}} + 740 \frac{1}{WL/(\mu\text{m}^2)} \frac{C_D^2}{(100 \text{ fF})^2} + 4000 \frac{1}{g_m/\text{mS}} \frac{C_D^2}{\tau/\text{ns}} (100 \text{ fF})^2$$

$$\text{ENC}^2 = a_{\text{shot}} \tau + a_{1/f} C_D^2 + a_{\text{therm}} \frac{C_D^2}{\tau}$$

$$\tau_{\text{opt}} = \left(\frac{a_{\text{therm}}}{a_{\text{shot}}} C_D^2 \right)^{1/2} = \left(\frac{4kT}{3eI_0 g_m} C_D^2 \right)^{1/2}$$



(a) Linear representation.



(b) Double logarithmic representation.

Pixel detector. As an example featuring small electrodes and correspondingly small input capacitances we choose a silicon pixel detector (section 8.7) with parameters $C_D = 200$ fF, $I_0 = 1$ nA, $\tau = 50$ ns, $W = 20$ μ m, $L = 0.5$ μ m, $g_m = 0.5$ mS, where we assumed a typical leakage current before the detector received substantial radiation damage. With (17.110) an equivalent noise charge of

$$\text{ENC}^2 \approx (24 e^-)^2(\text{shot}) + (17 e^-)^2(1/f) + (25 e^-)^2(\text{therm}) \approx (40 e^-)^2$$

Strip detector. For a typical silicon microstrip detector (see section 8.6.2) after radiation damage one obtains with $C_D = 20$ pF, $I_0 = 1$ μ A, $\tau = 50$ ns, $W = 2000$ μ m, $L = 0.4$ μ m, $g_m = 5$ mS:

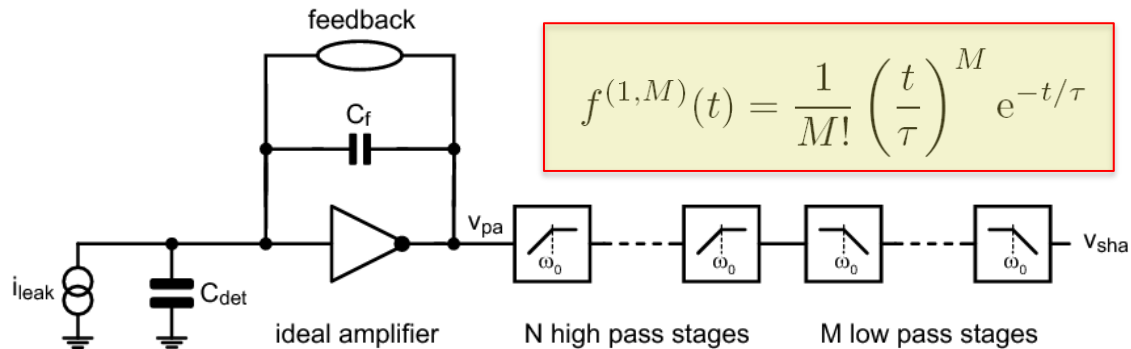
$$\text{ENC}^2 \approx (750 e^-)^2(\text{shot}) + (200 e^-)^2(1/f) + (800 e^-)^2(\text{therm}) = (1100 e^-)^2.$$

Liquid argon calorimeter. As an example of a detector with a large electrode capacitance we take a liquid argon calorimeter cell with typical values as given by the ATLAS electromagnetic calorimeter (see section 15.5.3.2 on page 597) in the central region. With the parameters $C_D = 1.5$ nF, $I_0 = < 2$ μ A, $\tau = 50$ ns, $W = 3000$ μ m, $L = 0.25$ μ m, $g_m = 100$ mS, i.e. assuming only a small (negligible) parallel shot noise (leakage current), one obtains:

$$\text{ENC}^2 \approx (1000 e^-)^2(\text{shot}) + (15000 e^-)^2(1/f) + (13500 e^-)^2(\text{therm}) \approx (20200 e^-)^2.$$

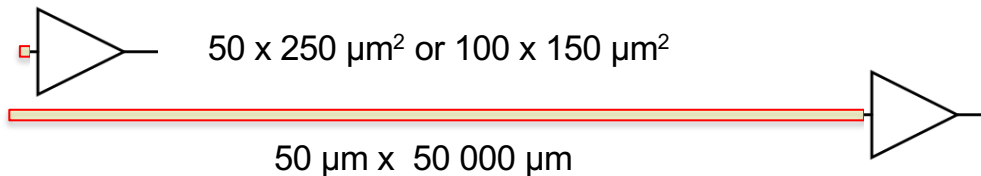
Noise in a pixel/strip/liq.Ar detector (ionisation detector)

... with CSA preamplifier & shaper



$$f^{(1,M)}(t) = \frac{1}{M!} \left(\frac{t}{\tau}\right)^M e^{-t/\tau}$$

comparing pixels
and strips



	C_D	I_0	τ	W	L	g_m	ENC therm	ENC 1/f	ENC shot	ENC tot
pixel	200 fF	1 nA	50 ns	20 μm	0.5 μm	0.5 mS	25 e ⁻	17 e ⁻	24 e ⁻	40 e ⁻
strip	20 pF	1 μA	50 ns	2000 μm	0.4 μm	5 mS	800 e ⁻	200 e ⁻	750 e ⁻	1100 e ⁻
liq. Ar	1.5 nF	2 μA	50 ns	3000 μm	0.25 μm	100 mS	1000 e ⁻	15 000 e ⁻	13 500 e ⁻	20200 e ⁻

- Rossi, Fischer, Rohe, Wermes, Pixel Detectors: from Fundamentals to Applications, Springer 2006
- Spieler, Semiconductor Detector Systems, Oxford Univ. Press. 2005
- Blum, Riegler, Rolandi, Particle Detection with Wire Chambers, 2010
- Leroy and Rancoita, Radiation Interaction in Matter and Detection, World Scientific, 4th ed, 2016
- Leroy and Rancoita, Silicon Solid State Devices and Radiation Detection, 2012
- Grupen and Shwartz, Particle Detectors, Cambridge Univ. Press, 2008
- Kolanoski, Wermes, Teilchendetektoren ... Grundlagen und Anwendungen (2016) in German
- Kolanoski, Wermes, Particle Detectors ... Fundamentals and Applications (2nd Edition in English, available in 2019)
- M. Garcia-Sciveres, N. Wermes, Review of advances in pixel detectors for experiments with high rate and radiation, Reports on Progress in Physics 81 (2018) no.6, 066101



UNIVERSITÄT

BONN